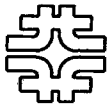

Fermilab MTF

Doc Number: MTF-96-0001
Version: 1.0
Category: MTF NOTE

MTF Single Stretched Wire System

J. DiMarco, J. Krzywinski *
Fermi National Accelerator Laboratory †
P.O. Box 500
Batavia, Illinois 60510

3/19/96

*associated with DESY and the Polish Academy of Sciences

†Operated by the Universities Research Association under contract with the U. S. Department of Energy

Contents

1 Introduction

A single stretched wire (SSW) system similar to that used at DESY for the HERA magnet measurements [1] has been developed to measure the integral strength ($\int gdl$) and centering parameters (center and roll angle) for the Fermilab Main Injector (FMI) quadrupoles at the Magnet Test Facility (MTF). The magnets have length $\sim 3m$, gradient of $\sim 23T/m$, and a large measurement aperture ($\sim 125mm \times 80mm$). The required accuracies are: strength to better than 5×10^{-4}, $x_0\ y_0 < 0.25mm$, and roll angle $< 0.5mrad$. This paper presents an overview of the SSW measurement system and its design considerations, anticipated performance, and recent results. Applications of the system to measurements of dipole magnets are also briefly discussed.

2 Description of Measurement Technique

Measurements with the SSW system consist in moving a single stretched wire in either x or y with the return wire held fixed either within the bore of the magnet or external to the magnet. The flux is given by

$$\begin{aligned} \Phi &= \int_{Area} \vec{B} \cdot \vec{da} \\ &= \oint_{closed\ loop} \vec{A} \cdot dl \end{aligned}$$

where $\vec{A}$ is the vector potential. The flux measured for the motion of a single wire therefore becomes

$$\Phi = L\ [A_z(x_2, y_2) - A_z(x_1, y_1)]$$

where

$$A_z = \Re \left[gR \sum_{n=1} \frac{b_n + ia_n}{n} \frac{1}{R^{n-1}} (x + iy)^n \right]$$

with definitions as below. The resultant change in flux will be independent of the path the wire takes from its initial to final position, and therefore, determination of the change in flux consists simply in measuring the integrated voltage as the wire moves from its start position (x_1, y_1) to its final position (x_2, y_2).

2.1 Conventions

The position of the wire in the SSW coordinate system will be given by x, y. The magnetic center of a quadrupole magnet is defined as the point within the quadrupole field which has zero dipole amplitude. A wire placed in a quadrupole field is displaced from magnetic center by a distance x_0, y_0, with the roll angle between the wire and magnet frames given by θ_r (see definitions in Figure 2). Considerations arising from the wire and magnet axes not being parallel and misalignments of the stage systems are considered separately. Where multipole harmonic coefficients are used, $n = 2$ indicates a quadrupole field and the coefficients have an additional phase of $n\theta_r$ as compared to the coefficients in the magnet frame (i.e. they are with respect to the SSW system). The harmonic coefficients of the magnet are defined as

$$b_n = \frac{C_n}{C_2}\cos(n\theta_n)$$

and

$$a_n = \frac{C_n}{C_2}(-1)\sin(n\theta_n)$$

where the C_n, R, and θ_n are the amplitude, reference radius, and phase of the harmonic fields respectively.

2.2 Basic flux measurements

A quadrupole field is given by

$$B_x = gy$$
$$B_y = gx$$

where g is the gradient at a reference radius R ($g = B_2/R$, where B_2 is the quadrupole field measured at R). For measurements in which a wire is moved in a *horizontal* plane aligned and centered in the quadrupole from position $x = 0$ to position $x = \pm D$, the flux is given by

$$\Phi_{H\pm} = \int V\,dt = \int B_y\,da = \int_0^{\pm D} g\,L_m\,x\,dx$$

where L_m is the magnetic length, x is the distance of wire travel (see Figure 2), and D is the $\pm$ limit of this travel. More generally, in the wire's frame, translated and rotated with respect to the magnet's,

$$\begin{aligned}\Phi_{H\pm} &= \int_0^{\pm D} g\, L_m \left[b_2\,(x - x_0) + a_2(y - y_0)\right] dx \\ &= L_m g \left[\frac{b_2}{2} D^2 \mp (b_2 D x_0 + a_2 D y - a_2 D y_0)\right] \qquad (1)\end{aligned}$$

($b_2 = \cos 2\,\theta_r$, $a_2 = \sin 2\,\theta_r$). Similarly for y motion from $y = 0$ to $y = \pm D$

$$\Phi_{V\pm} = L_m g \left[\frac{b_2}{2} D^2 \mp (b_2 D y_0 - a_2 D x + a_2 D x_0)\right]$$

The general flux expression for horizontal measurements, including all multipole fields, is given by

$$\Phi_{H\pm}(y) = L_m g R \left\{ \sum_{n=2}^{\infty} \left(\frac{1}{R}\right)^{n-1} \left[\frac{b_n}{n} \Re\{[(x - x_0) + i(y - y_0)]^n\} - \frac{a_n}{n} \Im\{[(x - x_0) + i(y - y_0)]^n\}\right]\right\}\Bigg|_0^{x=\pm D} \qquad (2)$$

(see [5]; note, however, the difference in notation in this reference).

2.3 Integrated strength determination

The quadrupole strength, gL_m can be determined from the basic flux measurements by

$$\Phi_{H+} + \Phi_{H-} = L_m g D^2\, b_2 \qquad (3)$$

and

$$\Phi_{V+} + \Phi_{V-} = L_m g D^2\, b_2$$

In our SSW system, for the purposes of saving costs, linear encoder systems were not purchased for the vertical motion stages, and so in practice the strength is accurately determined only from horizontal movement of the wire.

2.4 Centering parameters determination

Roll Angle: If we define a quantity x_0' by

$$\begin{aligned} x_0' &= -\frac{D}{2}\frac{(\Phi_H^+ - \Phi_H^-)}{(\Phi_H^+ + \Phi_H^-)} \\ &= x_0 b_2 + -2\, y\, \theta_r + 2\, y_0\, \theta_r \end{aligned} \tag{4}$$

the roll angle of the magnet with respect to the SSW system can be found by measuring x_0' as a function of the position y (note that the alignment requirement for roll angle (Section 6) allows $a_2 = -\sin 2\theta_r \approx -2\theta_r$ with negligible error). That is, since all other quantities are constants, the slope of x_0' vs. y in the SSW frame yields $-2\theta_r$.

Center Offsets: The centering parameters, x_0, y_0 are approximately determined by the same quantity measured at $x = 0,\ y = 0$

$$x_0' = -\frac{D}{2}\frac{(\Phi_H^+ - \Phi_H^-)}{(\Phi_H^+ + \Phi_H^-)} = x_0 b_2 + 2 y_0 \theta_r \tag{5}$$

$$y_0' = -\frac{D}{2}\frac{(\Phi_V^+ - \Phi_V^+)}{(\Phi_V^+ + \Phi_V^+)} = y_0 b_2 - 2 x_0 \theta_r \tag{6}$$

As will be shown, the θ_r terms are negligible.

2.5 Corrections for wire deflection

As is true for all measurements, strength, roll, and center offsets, the above measurements can be repeated at more than one tension and the results extrapolated to infinite tension if needed to remove effects from wire susceptibility, sag, etc. (see [1] for further discussion). In our application for the FMI magnets, these effects are small and measurements at multiple tensions are required only for determination of y_0 where the sag cannot be ignored.

2.6 Additional measurements

In addition to the measurement of quadrupole parameters described in this section, quadrupole axis determination and dipole measurements are briefly presented in Appendix C.

3 Description of System

The stretched wire system is comprised of precision motion stage units, supports for positioning and alignment of these units, ancillary components to support and tension the wire, and electronics and software for control and data acquisition. These systems are briefly described below. For reference, a list of SSW drawings, components, and a schematic diagram are given in Appendix A and Figure 1.

3.1 Hardware

3.1.1 Supports

Each end of the SSW system is composed of a base plate which is "permanently" fixed to the test stand, a highly rigid but removable fixture pinned to the base plate, and the stage unit which sits atop the fixture. The fixture supports the stage unit at three points (see Figure 3). The front spherical foot mates with a cup, while the back two are constrained to a groove or rest on a flat plate respectively. The spherical feet, coupled with the surfaces of the fixture and the bolts and spherical washers which can translate them, form a three point kinematic support which adjusts the position of the stage unit with respect to 5 axes: x, y, roll, pitch, yaw. After alignment, the bolts are tightened, and the position of the stage unit can be reproduced after removal and replacement of either the stage unit or stage unit plus fixture.

3.1.2 Stage units

The stage unit is comprised of precision $x - y$ stages (x–stage atop y–stage) mounted on a rigid angle bracket attached to a 1" thick Al stage unit plate. The stage unit plate is flat with respect to motion of the x–stage to better than $1mrad$ so that this surface can be used for roll angle alignment (Figure 6) (this was checked by establishing a line of sight parallel to the surface of the plate and measuring the position of the stage fiducials at $\pm$ maxima of stage travel). Also, the edge of the stage unit plate is perpendicular to the x–stage motion to within $1mrad$ for purposes of yaw alignment (Figure 6) (and similarly verified). Relevant features of the stages are summarized here:

- $\pm 1''$ travel, 25 pitch (0.040"/rev) stainless steel leadscrew
- straightness and flatness specifications: $< 1.5\mu m$

- $x - y$ orthogonality specification: $25\mu rad$
- x-stages equipped with $1\mu m$ accuracy linear encoders
- home and limit switches with $10\mu m$ repeatability (measuring this with the encoders indicates it is actually much better than this when approached slowly)

The stage unit is compact ($\sim 30 \times 30 \times 30cm$) and weighs $\sim$ 25kg and can be easily swapped for the stage unit at the other end of the test stand; as will be seen, this allows for more accurate determination of the roll angle. The SSW stage units are shown in Figure 4.

3.1.3 Stage tooling plates

Stainless steel tooling plates are pinned to the $6'' \times 6''$ surface of the stages. The wire support and tensioning systems are affixed to these plates. In addition, alignment fiducials are mounted directly on the tooling plates and an attempt has been made to align the edge fiducials parallel to the actual axis of stage motion (if this were the case, stage roll angle could be determined from these fiducials rather than from a μ-level). Figure 5 shows views of the tooling plates.

3.1.4 Wire support and tensioning

Stainless steel fixtures pinned to the stage tooling plates support the wire and tensioning system. The wear resistant wire guides (or 'jewels') are made of a hardened ceramic (Al_2O_3) and have been located to better than $\sim 10\mu m$ to the fiducials using a contour projector and $2.5\mu m$—accuracy height gauge. The wire support system strives to keep the wire in a well defined position while minimizing the distance of the wire support above the stage surface (important for minimizing stage error).

The wire used is CuBe, the advantage of which is a high strength to weight ratio (less sag) and lower paramagnetism than a material like tungsten. To remove any effects of sag, a tensioning system with stepping motor at one stage unit and tensoining gauge at the other, allows for measurements at several tensions which can then be extrapolated to infinite tension as was done at DESY [1]. At the tension motor end, a pulley is used so that the size of the tension motor does not dictate the wire distance above the stage surface. An arched metal spur on the tensioning motor shaft sleeve provides for quick, benign wire attachment (see Figure 5). At the tension

gauge end, a double set of jewels and G-10 post mounted directly in front of the gauge (moving axially on slides/pins) allows tension to be transmitted with no torque to the gauge. The G-10 post essentially provides a 'hook' with a moderate radius of curvature for attaching the wire. The wire comes off the jewels at both ends at a small angle ($\sim 50mrad$) so that the friction is minimized.

The wire supports are electrically isolated from the stage surfaces so that the system ground can be controlled. Connections of the wires to the input leads of the integrator are made on a section of copper rod (which provides thermal capacitance) thermally insulated within flasks (to reduce changes in thermovoltages) (Figure 3). This is necessary since the changes in thermovoltages create errors in the flux measurements (the constant offset voltage (drift) is subtracted).

3.2 Electronics

A Metrolab Precision Digital Integrator (PDI) is used to measure integrated voltage (flux) from the moving wire. The gain and linearity of voltage measured by the PDI has been calibrated against an HP3458A DVM to a few $\times 10^{-5}$ accuracy [3]. The cumulative integrated voltage is sampled at 15Hz, with triggers synchronized to the AC line cycle, and stored in the PDI resident memory until measurement end. A DVM measures the output of the magnet power supply current transductor as well as the output of the wire tension gauge. Motion control for the stages and tensioning motor is provided through Whedco drivers and translators via VME and GPIB. Output registers are used to control switch selection allowing for homing of individual stages and selection of operation mode (x, y, co-directional, counter-directional). Motions and pauses are made as fast as practical to minimize $1/f$ effects. (Typically stage motion is $\sim 5mm/s$ and the delay at each motion step $\sim 2s$ to allow wire oscillations to damp out). Closed loop feedback is used to control stage motion with measurement of actual distance traveled performed by the linear encoders.

3.3 Software

Currently the SSW system is used for production measurements of Fermilab Main Injector (FMI) magnets. These SSW measuremets use the database driven control and acquisition superstructure known as CHISOX [4] with the raw and analyzed data stored in SYBASE. CHISOX controls

all the motion, switching, and acquisition electronics allowing the measurements to be fully automated. Data acquired with CHISOX are not "real-time", and it is the analysis software which determines the start and stop times of stage motion from the data (see Section 8). Also, data acquisition can be performed using a UNIX shell-script (used during development of the system), and a MOTIF based GUI is being developed for 'stand-alone' SSW measurements.

4 Data Acquisition

4.1 Measurement description

SSW measurements begin with homing of the stages, so that a reproducible start position for survey and measurements is established. An optical or laser tracker survey is then performed to establish the location of the wire with respect to references on the magnet (see Section 7).

Measurements in x consist of starting the integrator with the wire stationary at $x = 0$, taking data for $\sim 2s$, moving the wire in $+x$ by a distance $D = 25mm$ at $\sim 5mm/s$ (pausing at D for $2s$ to allow oscillations time to damp), and returning to $x = 0$. After a $2s$ stop at zero, the wire is then moved in the same way in $-x$ with return back to $x = 0$. After three such cycles at a given current, integration is stopped and the integrated voltage vs. time data read from the PDI. The integrated voltage is sampled at 15Hz throughout the measurement cycles and current and tension are sampled at each start/stop position. With these x measurements, both the strength and x-center position can be determined (see Sections 2.3 and 2.4).

The y measurements are similar, but are typically performed at a single current since these measurements are only used for determining y-center position (independent of current). However, the measurements are repeated at several tensions to eliminate the effects of sag (see Sections 2.5, 5.3 9.4).

Roll angle determination consists of the x measurements above performed at $y = 0$, $+25mm$, $-25mm$ and combined as discussed in Sections 2.4 and 5.4. Again these measurements are typically performed at a single current. In addition, microlevel measurements of the roll of the stage units is needed (see Section 7.2).

Determination of the flux of each measurement is described in Section 8. Further measurement details are available in the procedure documentation [8].

4.2 Software and data storage

The CHISOX ([4]) check lists used for performing the above measurements are: *ssw_home_motors, ssw_scan_x, ssw_scan_y, ssw_roll_angle.* The check lists for data analysis are *analyze_ssw_strength, compare_ssw_survey,* and *correct_ssw_strength* (which corrects for the rather large octupole of the FMI quadrupole magnets). Data reduction for the analysis check lists is performed in the programs *reduce_and_record_ssw* and *red_ssw_scan_one_axis.* Raw flux data are stored in Sybase columns *flux_raw* and *t_flux* of flatcoil table *flatcoil_raw_pnts.* Reduced strength data are stored in flatcoil table *flatcoil_red_pnts.delta_integral_field_component.* Analyzed strength data (averaged and corrected) are stored in the results database table *magnet_strength.* Data pertaining to center, roll, and survey measurements are in tables *ssw_magnet_survey, ssw_jewel_survey,* and *ssw_survey_agreement* with survey data entered into the database using the script *ssw_magnet_survey.sh.*

5 Expected Errors

General requirements for system design were set forth in a previous document [2]. Here the focus will be on characterizing the SSW system which presently is in use. In estimating the error of a quantity which is a function of several variables, e.g. $f(x, y, z, \ldots)$, the following will be used:

$$(\Delta f)^2 = \left(\frac{\partial f}{\partial x}\Delta x\right)^2 + \left(\frac{\partial f}{\partial y}\Delta y\right)^2 + \left(\frac{\partial f}{\partial z}\Delta z\right)^2 + \ldots \qquad (7)$$

5.1 Stage errors

A sketch defining the various axes of a stage is given in Figure 7. The performance of a stage is usually characterized according to deviations in straightness and flatness over its travel. These are usually measured by mounting a laser interferometer target at some height above the stage and recording these deviations as a function of travel. These straightness and flatness errors, however, are not uniform translations of the entire stage in x, y, z, but rather stem from imperfections in the stage which allow its pitch, yaw, and roll angles to change as it travels. Knowledge of these angles is useful in calculating positioning errors caused by the stages. For the SL2002 stages used in the SSW system, PPL indicated that the pitch, yaw, and roll of the stages were better than $25\mu rad$ over an inch of travel.

Using these, the errors in wire motion during SSW measurements can be estimated. As shown in Figure 7, because the wire is supported a distance off the stage surface, it is the pitch error which causes an error in the distance traveled by the stage. The stage platform (the travel of which the encoder would measure) might move exactly D but that because of the pitch angle error, the wire would move less than that. Since the SSW is supported off the stage by a distance of no more than $\sim 50mm$ at either stage, we will use $H = 50mm$ to estimate this error. This implies

$$\begin{aligned} \Delta x &= H\,\theta_{pitch_{stage}} \\ &= 1.25\mu m \end{aligned} \tag{8}$$

This error is consistent with the stage certification that PPL performed comparing the encoder readout to an optical master.

Straightness errors should be given by

$$\Delta y = H\theta_{roll_{stage}} + W\theta_{yaw_{stage}} \tag{9}$$

where H is the height above the stage and the W used depends on the the point about which the stage is yawing (if yawing about the center, W is effectively zero). Choosing W as half the width of the stage (76mm) (i.e. the axis of yaw is a corner), and H as above, Δy is expected to be $3\mu m$. Since this is somewhat larger than the stage specification ($1.5\mu m$), W or the angles, are better than this.

5.2 Strength error

Assuming that the roll, yaw, and pitch of the SSW system relative to the magnet have been adjusted according to the requirements in Section 6 (and therefore cause negligible error), an estimate of the error in measured quadrupole strength from Eqns. 3 and 7 can be expressed as

$$(\Delta L_m g)^2 = \left(\frac{1}{D^2}\Delta\Phi^+\right)^2 + \left(\frac{1}{D^2}\Delta\Phi^-\right)^2 + \left(\frac{-2(\Phi^+ + \Phi^-)}{D^3}\Delta D\right)^2$$

Furthermore, if the wire is reasonably centered in the field, $\Phi^+ \approx \Phi^- \equiv \Phi$, then the error in either $\pm$ flux measurements is $\Delta\Phi$ and the above becomes

$$(\Delta L_m g)^2 = 2 \times \left(\frac{1}{D^2}\Delta\Phi\right)^2 + \left(\frac{4\Phi}{D^3}\Delta D\right)^2 \tag{10}$$

The relative error of the strength measurement is thus given by

$$\left(\frac{\Delta L_m g}{L_m g}\right)^2 = 2 \times \left(\frac{\Delta \Phi}{2\Phi}\right)^2 + \left(\frac{2\Delta D}{D}\right)^2 \tag{11}$$

Estimate of Systematic Error: Since the calibration and linearity of the PDI integrator used for flux measurement is accurate at the level of $\sim 10^{-5}$, the systematic error in strength determination is governed by ΔD (the error in measurement of wire position) and other factors such as multipole errors, and measurement of magnet current.

The systematic ΔD should stem mainly from the imperfections in the individual stages (note that a factor of $\sqrt{2}$ is gained since both ends would have to cooperate to generate this overall error). Since ΔD from the stages was estimated in Section 5.1 as $1.25\mu m$, the estimated accuracy of the system for a move of $D = 25mm$ would be

$$\begin{aligned}\left(\frac{\Delta L_m g}{L_m g}\right) &= \left(2 \times \frac{\sim 1 \times 10^{-6} m}{0.25 m}\right) \\ &= 0.8 \times 10^{-4}\end{aligned}$$

By calibrating the stage motion near the position of the wire with an interferometer, this accuracy can be checked. The results of such a calibration are presented in Section 9. Note that since the start and stop positions at both ends of the wire are measured, the proper effective wire motion can be determined with negligible error in the strength calculation (see Appendix B).

The first order errors arising from multipoles cause the measured strength, $(L_m g)'$, to differ from the actual strength by

$$L_m g' - L_m g = \frac{b_4}{2}\frac{D^2}{R^2} + \frac{b_6}{3}\frac{D^4}{R^4} + \ldots \tag{12}$$

and can be removed using the calculated influence from measured multipoles or through additional measurements as discussed in [5]. For $x_0,\ y_0 \neq 0$, additional multipole errors (to powers of $\left(\frac{\delta}{R}\right)^2$ (δ being either of $x_0,\ y_0$) and $n \leq 6$) are

$$\begin{aligned}L_m g' - L_m g \;=\; & -2b_3\frac{x_0}{R} + 2a_3\frac{y_0}{R} + 3b_4\frac{x_0^2 - y_0^2}{R^2} - 6a_4\frac{x_0 y_0}{R^2} - 2b_5\frac{D^2 x_0}{R^3} + \\ & 2a_5\frac{D^2 y_0}{R^3} + 5b_6\frac{D^2\left(x_0^2 - y_0^2\right)}{R^4} - 10a_6\frac{D^2 x_0 y_0}{R^4}\end{aligned} \tag{13}$$

For multipoles smaller than a few units (measured at R) and x_0, $y_0 < 0.1 \times R$, these additional contributions are negligible.

Effects from slight paramagnetism of the wire are potentially significant and can be removed by performing measurements as a function of tension. At DESY, paramagnetic effects accounted for an error of 2×10^{-4} in the strength [1] however this effect is negligble for FMI magnets which have a lower gradient and require a shorter wire span (see Appendix D).

The transductor which measures magnet current has a calibration which is known in relation to other devices: its absolute accuracy, however, is not well known.

Random Errors: The main sources of random error in the SSW measurements of strength are RMS variation in encoder readout (not actual position variation), vibrations, electrical noise, and power supply readout instabilities. Unmeasured wire motion (e.g. from wire slippage on the jewels) is believed to be negligible (see Section 8).

To estimate the RMS error from the encoder we need only estimate the error in the effective D measured by the encoders assuming the $\pm$ positions reported at each end have an RMS error of the least encoder count ($1\mu m$). Since these four quantites are averaged to determine a D_{eff} (Appendix B), the ΔD_{eff} is just $0.5\mu m$ and leads to a relative strength error of

$$\left(\frac{\Delta L_m g}{L_m g}\right) = \left(\frac{2\Delta D}{D}\right) \simeq 0.5 \times 10^{-4}$$

for $D = 25mm$.

Wire vibrations for the FMI quadrupole measurements at MTF, experimentally appear to be $\sim 1\mu m$. These give rise to fluctuations in measured flux, $\Delta L_m g D^2$, of $2L_m g D \Delta D$ (see Eqn. 11), or for FMI quadrupoles at 3kA ($L_m g = \sim 50T$), about $2\mu V - s$. A sample of relative data fluctuations at 3kA with the wire stationary at three of its 'flattops' is shown in Figure 8. For the most part, the higher frequency mechanical vibrations shown in the figure average out since many points are sampled at each flattop, and it is the low frequency electrical noise which dominates the error in determining flux.

In the present setup, the limit of our ability to accurately measure the flux in the electrical noise environment at MTF is $\sim 1 - 2 \times 10^{-6} V - s$ (Section 8). Using Eqn. 10 and motion of $25mm$, this gives rise to random

errors on the order of

$$\begin{aligned} \Delta L_{mg} &= \frac{2\,\Delta\Phi}{D^2} \\ &= 0.003\,T \end{aligned}$$

For FMI measurements at $2kA$, $\Phi = 10mV - s$, and the relative random error is

$$\begin{aligned} \left(\frac{\Delta L_{mg}}{L_{mg}}\right) &= \left(\frac{\Delta\Phi}{2\Phi}\right) \\ &= \sim 1 \times 10^{-4} \end{aligned}$$

The stability of the power supply and current measurement, of course, directly affect the RMS variation in measured strength.

5.3 Offset determination error

With measurement at $y = 0$, x_0 is estimated from

$$\begin{aligned} x_0' &= -\frac{D_{eff}}{2}\frac{(\Phi_H^+ - \Phi_H^-)}{(\Phi_H^+ + \Phi_H^-)} \\ &= x_0 + 2\,y_0\,\theta_r \end{aligned} \tag{14}$$

and the error in x_0' can be expressed as

$$(\Delta x_0')^2 = \left(\frac{\partial x_0'}{\partial \Phi^+}\Delta\Phi^+\right)^2 + \left(\frac{\partial x_0'}{\partial \Phi^-}\Delta\Phi^-\right)^2 + \left(\frac{\partial x_0'}{\partial D_{eff}}\Delta D_{eff}\right)^2 \tag{15}$$

where D_{eff} is the effective wire motion (see Appendix B). The error in determination of centering parameters is generally very small in comparison to transferring this determination to a reference surface on the quadrupole. For situations where such effects may be relevant (e.g. relative measurements), sources of error including alignment, motion errors, flux measurement errors, and multipole contributions are discussed below.

Systematic Errors: Causes of systematic errors in offset determination include alignment, errors in D_{eff}, multipoles, and sag effects.

The systematic error in x_0' caused by a non-zero roll angle is small: $\sim 4\mu m$ (assuming $y_0 \leq 0.002m$, $\theta_r \leq 0.002mrad$ as described in Section 6).

Accurate measurement of D_{eff} is not a concern in the offset measurements; though the last term in Eqn. 15 involves errors in D_{eff}, x_0' is very insensitive to those errors (e.g. with the wire off center by $2mm$ and a $10\mu m$ error in D_{eff}, the error is $< 1\mu m$).

The presence of multipole fields causes a small error (on the order of few μm's). For example, the leading multipole errors cause x_0' to differ from x_0 by

$$x_0' - x_0 = -\frac{b_3}{3}\frac{D^2}{R} + \frac{(x_0 b_4 - y_0 a_4)}{R}\frac{D^2}{R} - \frac{b_5}{5}\frac{D^4}{R^3} + \frac{(x_0 b_6 - y_0 a_6)}{R}\frac{D^4}{R^3} \quad (16)$$

or similarly for the $y-$direction

$$y_0' - y_0 = \frac{a_3}{3}\frac{D^2}{R} + \frac{(-x_0 a_4 - y_0 b_4)}{R}\frac{D^2}{R} - \frac{a_5}{5}\frac{D^4}{R^3} + \frac{(x_0 a_6 + y_0 b_6)}{R}\frac{D^4}{R^3} \quad (17)$$

Sag does not influence the x_0' measurements but is a large, $\sim 75\mu m$ error, for FMI y_0' (see Appendix D). The elimination of the sag depends on the fit of y_0' as a function of $\frac{1}{T}$ and so depends on the number of tensions measured, the linearity and stability of the tension gauge, and frictional effects (the gain calibration does not affect the result). When non-linearities in the y_0' vs. $1/T$ data occur, the uncertainty in the y_0' determined from extrapolation is on the order of $10 - 20\mu m$.

RMS Errors: Near magnet center $\Phi^+ = \Phi^- \equiv \Phi$ and so combining the flux terms in Eqn. 15 gives

$$\Delta x_0' = \frac{1}{\sqrt{2}}\left(\frac{D_{eff}}{2}\right)\frac{\Delta\Phi}{\Phi} \quad (18)$$

which serves as an estimate of the variation in x_0' expected from errors in measurement of flux. For example, for $\Delta\Phi \sim 2 \times 10^{-6} V - s$, $\Phi = 10mV - s$ (FMI at 2kA), $D_{eff} = 25mm$, the RMS variation expected is $\sim 2\mu m$.

Also, as discussed in Appendix B, $x-$stage errors, random encoder errors, wire slippage on the jewels and other errors which cause a disparity in $\pm$ movements all cause errors in determining x_0'; the error being the motion disparity itself. For x_0', where there are encoders, this type of error is very small ($1-2\mu m$). For y_0', however, where the $\pm$ distances are assumed equal to their nominal values, stage travel may be disparate by $5 - 10\mu m$ (depending on the reproducibility, this may instead result in a systematic error to the measurements).

With RMS variation of the tension gauge $\sim$ 20 grams, removing wire sag influence with extrapolation of the $1/T$ data (taking three measurements at each of three tensions) gives an uncertainty on the intercept of the fit of about $3 - 5\mu m$ for a typical measurement.

5.4 Roll angle determination error

The simplest roll measurement would involve measuring x_0' at $y = \pm D$ (see e.g. Figure 2) and using Eqn. 4 to determine the slope, $-2\theta_r$, from

$$-2\,\theta_r \;=\; \frac{x_0'(D) \;-\; x_0'(-D)}{2D}$$

This implies

$$\theta_r = \frac{-\delta}{4D} \tag{19}$$

where $\delta = x_0'(D) \;-\; x_0'(-D)$. The error in this quantity can be estimated as

$$(\Delta\theta_r)^2 \;=\; \frac{(\Delta\delta)^2}{(4D)^2} + (\theta_r)^2 \left(\frac{\Delta D}{D}\right)^2 \tag{20}$$

The term with $\frac{\Delta D}{D}$ is not a significant contribution (e.g. if $\theta_r = 10mrad$, $D = 25mm$, $\Delta D = 10\mu m$ this term amounts to $4\mu rad$) and is why encoders for the y stages are not necessary. Thus the error in roll angle depends entirely on the error of δ, the difference of the measured x_0''s. The chief factors which could create an error in this difference are

- **$x-y$ stage orthogonality:** An error in stage perpendicularity creates an offset in the x_0' at one y extreme relative to the other by $\Delta x_0' = 2D\Delta\theta_{orthog}$. The stage orthogonality specification is $25\mu rad$ which implies an error of $\Delta\delta = 1.25\mu m$.

- **straightness of $y-$stage over full travel:** If the $y-$stage has imperfections in its travel from $y = D$ to $y = -D$, error will be incurred in the measurement of δ. From Eqn. 9 the straightness error incurred by the $y-$stage should be given by

$$\Delta x = (H + T)\theta_{roll_{stage}} + W\theta_{yaw_{stage}}$$

where the total height of the wire above the stage, $H + T$ (H is the height of the wire support above the stage surface ($\sim 50mm$) and T is the thickness of the $x-$stage ($\sim 75mm$)) is used. With $W = 76mm$ as before, and specifications of $\theta_{roll_{stage}} = \theta_{yaw_{stage}} = 25\mu rad$, these terms yield an error of $\Delta\delta = 5\mu m$.

- **multipole induced errors:** The dominant error from multipole fields stems from the dodecapole (12-pole), the influence of which changes sign at $\pm y$ so that its effect is additive. This multipole gives rise to an error in measured roll angle, θ'_r, of

$$\theta'_r - \theta_r = \frac{-1}{2}\left(a_6\frac{D^4}{R^4} + a_6\frac{c^4}{R^4} - a_6\frac{10}{3}\frac{D^2c^2}{R^4}\right) \tag{21}$$

where $\pm c$ are the y positions at which x'_0 is measured. If $c = D$ is chosen, this implies

$$\theta'_r - \theta_r = a_6\frac{2}{3}\frac{D^4}{R^4}$$

For the Fermilab Main Injector, the 0.6 unit skew dodecapole yielded an error in roll angle of $\sim 40\mu rad$ (error of $\Delta\delta = 4\mu m$) (the next multipole to contribute is a_{10}, which for $y = \pm D$ yields an error of $a_{10}\frac{8}{5}\frac{D^8}{R^8}$).

Additional multipole terms may contribute if the wire is not centered in the magnet (x_0, $y_0 \neq 0$). The lower order terms (through $n = 7$) yield an additional error in θ'_r of

$$\begin{aligned}\theta'_r - \theta_r = b_3\frac{y_0}{R} + a_3\frac{x_0}{R} - a_4\frac{3}{2}\frac{x_0^2 - y_0^2}{R^2} - 3b_4\frac{x_0y_0}{R^2} + \\ -4a_7\frac{x_0}{R}\left(\frac{D^4}{R^4}\right) + -4b_7\frac{y_0}{R}\left(\frac{D^4}{R^4}\right)\end{aligned} \tag{22}$$

For example, the FMI quads have $b_4 \sim 5$ units. If $x_0 = y_0 = 2.5mm$, these add an additional $15\mu rad$ error. For a magnet with small unallowed multipoles or a wire that is adequately centered, these additional effects can be ignored.

All multipole effects, however, are calculable and can be removed during analysis if the multipole fields are known.

- **measurement error in x_0'**: Any systematic error contribution to measurement of x_0' (except multipoles) should be present at all y positions and therefore should not effect the slope (i.e. θ_r) determination. However, non-flux-related RMS errors such as discussed in the previous section, may contribute $\sim 2\mu m$ to the error in δ.

- **errors from flux measurement**: Errors in the determination of flux can affect the measurement of x_0' according to Eqn. 18. If only the two $y = \pm D$ positions are measured then the error in δ would be $\sqrt{2}$ times the error estimate given in this equation. For an error in flux of $2 \times 10^{-6} V - s$, this implies an RMS error in δ of $\sqrt{2}\Delta x_0' = 3\mu m$.

Summing these errors gives a total error in δ of $\sim 12\mu m$ assuming multipole errors are removed. Using Eqn. 19 this works out to $120\mu rad$ error in the θ_r for $D = 25mm$.

This basic accuracy can be improved, however. The stage units are small and light enough to be swapped end-for-end relative to the magnet to repeat the measurement of roll angle. If the stage units are aligned relative to gravity in the same way for both the original and swapped positions (see Section 7), then θ_r measured in the original configuration should equal $-1 \times \theta_r$ in the swapped position. Since the offset caused by the motion and quality of the stages will not change sign with the swap, the roll angle offset caused by the stage units can be determined and removed. Of the errors listed above this includes orthogonality and straightness errors of the stages.

6 Alignment

There are five coordinate axes of concern in setting up the SSW system relative to the magnet: x, y, roll, pitch, yaw as shown in Figure 9. This is true of both of the $x - y$ stage units comprising the SSW system. This section aims at providing the *minimal* alignment requirements needed to satisfy the FMI requirements of measurement accuracy. Transfer of the measured parameters, x, y, θ_r, from the SSW system to magnet fiducials is discussed in the next section.

6.1 Translation alignment (x_0, y_0):

If one or both ends of the SSW system are translated in x, y, the result is that the wire has an average displacement, or is at an angle, relative to the

magnet's axis. This has been shown to negligibly effect the strength determination (see Appendix B and Eqns. 12, 13), and also has little influence on determination of the centering parameters (Eqns. 14, 16, 17) or roll angle (Eqn. 22). Thus, requiring

$$x_0,\ y_0 < 2mm \tag{23}$$

for the FMI measurements allows translation errors in either or both stage units to be ignored.

6.2 Roll angle alignment:

θ_r affects the strength determination according to Eqn. 3. That is, the strength is determined from

$$\begin{aligned} L_m g &= \frac{\Phi_{H+} + \Phi_{H-}}{D^2 \cos(2\theta_r)} \\ &\approx \frac{\Phi_{H+} + \Phi_{H-}}{D^2 \left(1 - 2\theta_r^2\right)} \\ L_m g \left(1 - 2\theta_r^2\right) &\approx \frac{\Phi_{H+} + \Phi_{H-}}{D^2} \end{aligned}$$

Therefore, if the error in strength, $2\theta_r^2$, is to be kept less than 0.5×10^{-4}, this requires

$$\theta_r < 5 \times 10^{-3} \tag{24}$$

This requirement is achieved practically by leveling the magnet, and leveling each individual stage unit using a microlevel on each stage unit plate (assuming that the degree of parallelness between the stage and the stage unit plate is known - see Section 3). The measurements of θ_r and x_0, y_0 are rather insensitive to roll angle alignment (Sections 3.4 and 5.3).

6.3 Stage yaw alignment:

A yaw angle in either or both stage units relative to the magnet axis effects the actual distance the stage moves in the x direction. Yaw errors cause the distance of wire travel, D_{eff}, to have a factor $\cos\theta_{yaw} \approx 1 - \frac{1}{2}\theta_{yaw}^2$. An error in D_{eff} has little effect on the roll or center offset determinations (Sections 5.3 and 5.4), and so it is the strength measurement which again drives the

requirement. Since the relative strength error from ΔD_{eff} is given by $\frac{2\Delta D}{D}$ (Eqn. 11), maintaining an error in strength $< 0.5 \times 10^{-4}$ requires

$$\frac{2\Delta D}{D} = \frac{2\left(D \times \frac{1}{2}\theta_{yaw}^2\right)}{D} < 0.5 \times 10^{-4}$$

that is,

$$\theta_{yaw} < 7\ mrad \tag{25}$$

By establishing a line of sight parallel to the magnet axis (using external fiducials of the magnet) and measuring the distance from the line of sight to positions at the side of each stage unit plate, θ_{yaw} can be measured and adjusted. This assumes that the edge of the stage plate is perpendicular to the axis of travel of the stage to an acceptable amount (see Section 3).

6.4 Stage pitch alignment

A non-zero pitch in a stage unit affects the y_0 and θ_r determinations by altering the D_{eff} for y motions by a factor $1 - \frac{1}{2}\theta_{pitch}^2$. The relative accuracy required for y_0 and θ_r measurements is not very high: if require θ_r measurement $< 20\mu rad$ and alignment requirement is $5mrad$ (Eqn. 24), this implies 4×10^{-3} accuracy; if require y_0 measurement to $5\mu m$ and alignment requirement is $2.5mm$ (Eqn. 23), this implies 2×10^{-3} accuracy. Since the relative error in both y_0 and θ_r that is caused by the distance error is given by $\frac{\Delta D}{D}$ (Eqns. 15 and 20), measurements require

$$\frac{\Delta D}{D} < 0.002$$

where the ΔD caused by pitch misalignment is $\frac{D}{2}\theta_{pitch}^2$. This implies

$$\theta_{pitch} < 60\ mrad \tag{26}$$

which is easily accomplished.

7 Transfer of Centering Parameters

If the alignment requirements above are met, the SSW system can determine the x_0, y_0, θ_r to accuracy as described in Section 5. These accuracies are related to the SSW system , however, and must be transferred to magnet fiducials to be useful during magnet installation. The transfer process incurs its own set of errors which add to the system inaccuracies previously discussed.

7.1 Error in Transfer of x_0, y_0

Wire location relative to SSW fiducials: The SSW stage units have fiducial 'nests' mounted on them to facilitate transfer of the x_0, y_0 coordinates measured. The nests are made to hold a laser tracker retro-reflector (which will be used during installation of the Main Injector magnets) but have an adapter so that they can be used with optical survey equipment which is more readily available at MTF. The x, y offset between the center of a survey ball or retro-reflector at the nest and a wire on the ceramic jewel requires calibration. This was accomplished using a contour projector to first transfer the position of the wire as it rests on the jewel to one of the pinned mounting plates on the tooling plate surface, and then using a precision distance caliper to determine the distance from the mounting plate to the center of the survey ball. This procedure could be used to locate the wire to the nest within $\sim 10\mu m$. However, the radius of the jewel groove was chosen to be $100\mu m$ (to minimize abrasion on the wire and to allow flexibility in choosing larger diameter wires), and so with the wire radius typically used being $50\mu m$, there may be an additional $\sim 25\mu m$ uncertainty in the wire location on the jewel.

Influence of Fixture Positioning: If the $x-y$ stage units of the SSW system are not close to the magnet ends *and* the wire is not parallel to the magnet axis, transfer errors on the order of 10's of μm can result because the stage locations do not adequately represent the location of the wire at the magnet end. For example, if the x–offset of the wire at one end of a $2.5m$ magnet is $2mm$ (a $800\mu rad$ angle) as shown in Figure 10, the stage holding the wire $10cm$ from the magnet will be further translated, relative to the magnet axis, by $\Delta x = 80\mu m$. In the figure, if the distances from stages to magnet, p and q are the same, then when measurement of both stage fiducials are combined, the net effect is zero. If these are not the same, the

wire would have to be near parallel with respect to the magnet axis to avoid this type of error; this can be achieved either through alignment of the wire using magnet fiducials, or by determining the magnet axis (see Appendix C). Note that since this effect is a constant, determination of roll angle from x_0''s at different y locations is not affected.

Measurement of SSW and Magnet Fiducials: Measuring the distance from the fiducial nests to the magnet fiducials is presently accomplished via optical survey or using a laser tracker. The laser tracker accuracy is nominally $50\mu m$ while optical survey is typically $\sim 125\mu m$. Given the above errors, these transfer techniques provide sufficient accuracy for current applications of the system.

7.2 Error in transfer of θ_r

The roll angle measured, θ_r, is transferred by relating the roll of the SSW system and the roll of the magnet to gravity.

Magnet Roll: The roll of the magnet with respect to gravity must be determined from its fiducials. For the FMI, targets (survey scales or a retroreflector) are placed at several locations on the exposed lamination surfaces at the top of the magnet, and the differences in height of the the targets is determined using a laser tracker or optical survey. The lamination surface openings are separated in x by $\sim 400mm$ so that for y measurement error $\sim 100\mu m$, θ_r can be measured with error $\sim 200\mu rad$.

SSW System Roll: The SSW measurement of magnet roll angle is performed by first determining the roll angles of the stage unit plates at both ends of the system using a microlevel, and then performing a measurement of roll angle as described in Section 2. The roll angle can be found from

$$\theta_r = \theta' - \theta_m + \theta_l - \theta_e \tag{27}$$

where

- θ_r is the roll angle of the magnet with respect to gravity and is the quantity of interest
- θ' is the angle determined from measurements (e.g., as described by Eqn. 19) with errors as described in Section 5.4

- θ_m is the offset arising from multipoles (this can be calculated)
- θ_l is the angle of stage unit platforms mesured with microlevels before each SSW roll measurement
- θ_e is the system offset present (determined via calibration as described below) caused by
  - errors in the stages (including $x-y$ stage perpendicularity, straightness, etc.)
  - the stage unit plates (where the microlevels are placed to read θ_l) not being perfectly parallel with respect to the $x-$stage motion

(Note that the offset of the microlevel is not included as a factor, since the offset is checked periodically by measuring with 0° and 180° on a flat granite table. Moreover, a single microlevel is used, reading first one stage unit plate and then the other; since the two stage units face each other during measurements, any offset in the level will cancel when the two readings are averaged to determine θ_l).

Transfer errors in the roll angle measurement are incurred both by θ_l and θ_e in Eqn. 27 since both these quantities use microlevel readings to relate the angle of the system to gravity. The error in reading the microlevel is $\sim 25\mu rad$, and since the offset has effectively been removed, this serves as an estimate of all θ_l measurements.

To determine θ_e, a roll angle measurement is first made with θ_l adjusted to be zero for each stage unit. The stage units are then swapped end for end, the stage unit plates again leveled to zero, and the magnet roll angle remeasured. The first roll angle measured (Eqn. 27) is

$$\theta_r = \theta' - \theta_m - \theta_e$$

and the seconds is

$$\theta_r = \theta'' - \theta_m + \theta_e$$

Combining these equations allows determination of

$$\theta_e = \frac{1}{2}\left(\theta' - \theta''\right) \tag{28}$$

Thus, determination of θ_e involves the average of (at least) two θ_l measurements and two roll angle measurements (normal and swapped positions)

with inherent random errors as described above for θ_l and in Section 5 for θ'. For the FMI measurements, this gives an expected error in θ_e of $\sim 40\mu rad$ for a single calibration.

An estimate for transfer error of a single roll measurment would be the uncertainty of a θ_l measurement combined in quadrature with the above error in θ_e determination: this yields an RMS error of $\sim 50\mu rad$.

8 Determination of Flux

8.1 Method

A single flux motion step is shown in Figure 11, where $\Phi(t) = \int_0^T V(t)dt$. The wire is at rest at $t = 0$, begins motion at $t = t_1$ and arrives at its final position at $t = t_2$, where oscillations are allowed to damp for $\sim 2s$. Similarly, times t_3, t_4 give the times of return motion. The constant slope or 'drift' observed is caused by the integration of a constant offset voltage present in the electronics (PDI) or stemming from thermovoltages in the connections from the integrator to the stretched and return wires. To determine the flux caused by wire motion through the magnetic field, three distinct regions where the wire is at rest are determined for each flux motion step. The points t_0, t_2, t_4 are determined from the data by performing a linear least squares fit to a specified number of points (for FMI 30 points are used) starting at each point, and searching for regions where the errors in the fitted slope are a minimum (see Figure 12). The slopes starting at these points, s_{t0}, s_{t2}, s_{t4} measure the voltage offset in the system and provide information on the offset variation. The average offset is subtracted, leaving the corrected measured flux, y_{cor}, according to

$$y_{cor}(t) = y(t) - m_d t \tag{29}$$

(where m_d is the average of s_{t0}, s_{t2}, s_{t4}) and the flux determined from

$$\Phi = \frac{1}{N}\sum_{n=0}^{N-1} y_{cor}(t_2 + n\Delta t) - \frac{1}{2}\left(\frac{1}{N}\sum_{n=0}^{N-1} y_{cor}(t_0 + n\Delta t) + \frac{1}{N}\sum_{n=0}^{N-1} y_{cor}(t_4 + n\Delta t)\right) \tag{30}$$

with $1/\Delta t$ being the sampling frequency ($\sim 15Hz$) and N is the nominal number of 'good' points at flattop (e.g. 30 points for a two second wait at flattop).

8.2 Noise considerations

Efforts have been made to reduce the effects of noise by thermally stabilizing wire connections, making motions as quickly as practical, synching sampling triggers with $60Hz$ line and $15Hz$ booster frequencies, and using a ferrite ring on the signal inputs to the PDI (to reduce rectified high frequency noise).

8.2.1 Expected influence

Assume that

$$\begin{aligned} t_0 &= t_2 - T \\ t_4 &= t_2 + T \end{aligned}$$

as shown in Figure 11. The voltages stemming from noise at frequency ω can be expressed as

$$V_\omega(t) = A(\omega)e^{i\omega t} \tag{31}$$

and its resultant flux as

$$\Phi_\omega(t) = \frac{1}{i\omega}A(\omega)e^{i\omega t} \tag{32}$$

where $A(\omega)$ is the amplitude of the noise at the frequency ω and the phases are assumed random. With Eqns. 30 and 32 the noise contribution to a determination of a flux step can be written as

$$\begin{aligned} \Phi_{noise}(\omega) &= \frac{1}{N}\sum_{n=0}^{N-1}\frac{A(\omega)}{i\omega}e^{i\omega(t_2+n\Delta t)} - \\ &\quad \frac{1}{2}\left(\frac{1}{N}\sum_{n=0}^{N-1}\frac{A(\omega)}{i\omega}e^{i\omega(t_2-T+n\Delta t)} + \right. \\ &\quad \left. \frac{1}{N}\sum_{n=0}^{N-1}\frac{A(\omega)}{i\omega}e^{i\omega(t_2+T+n\Delta t)}\right) \end{aligned}$$

which simplifies to

$$\begin{aligned} \Phi_{noise}(\omega) &= \frac{A(\omega)}{i\omega}\, e^{i\omega t_2}\, \left[2\sin^2\left(\frac{\omega T}{2}\right)\right] \frac{1}{N}\sum_{n=0}^{N-1} e^{i\omega n\Delta t} \\ &= \Phi_\omega(t_2)\, 2\sin^2\left(\frac{\omega T}{2}\right) \frac{1}{N}\sum_{n=0}^{N-1} e^{i\omega n\Delta t} \end{aligned} \tag{33}$$

The worst case frequency is where $\frac{\omega T}{2} = \frac{\pi}{2}$, that is, where $f = \frac{1}{2T}$. For the speed of our stage motions ($\sim 5mm/s$) and length of flattop duration $\sim 2s$ this implies a frequency of $\sim 0.15Hz$. The RMS flux error from all frequencies of noise would be

$$\Phi_{RMS} = \sqrt{\sum_{\omega} A^2(\omega)\frac{4}{\omega^2}\sin^4\frac{\omega T}{2}\left(\frac{1}{N}\sum_{n=0}^{N-1} e^{i\omega n\Delta t}\right)^2} \tag{34}$$

Note that the factor $\frac{1}{N}\sum_{n=0}^{N-1} e^{i\omega n\Delta t}$ (stemming from averaging over the flattops) is useful in helping to reduce higher frequency noise effects; for the worst case frequency, $f = \frac{1}{2T}$, however, the reduction is only $\sim 0.3\%$ of the RMS error contribution.

The Φ_ω spectrum caused by the MTF noise background (averaged over 20 measurements) is shown in Figures 13 and 14 for measurements made with the PDI inputs shorted and with the SSW system attached (the wire being in a low field region (magnet center) with zero movement at 0A). Applying the amplitudes and frequencies in these background measurements according to Eqn. 34 yields an expected Φ_{RMS} of $0.6\mu V - s$ and $2.6\mu V - s$, with the PDI shorted or wire attached respectively, for flattops separated by $T = 7s$. In adding two flux steps (from $\pm$ motions) the t_0's of which are separated by time $2T$ (Figure 11), the Φ_{RMS} expected is $0.4\mu V - s$ with the PDI shorted and $1.7\mu V - s$ with the SSW attached.

8.2.2 Experimental noise results

Experimentally, RMS variation of flux measurements taken under various circumstances are summarized in Figure 15. Based on these measurements the noise from the system as a whole would seem about three times worse than the noise of the PDI itself. Since the variations are independent of current and are present with or without stage operation, they would seem to stem from sources other than:

- power supply
- wire vibration/slip
- stage motors
- thermovoltage variations in wire connections

As demonstrated by measurements G and H in Figure 15, making measurements as quickly as possible (tempered by the desirability of limiting wire vibrations), reduces Φ_{RMS} because of the $1/f$ decrease in noise amplitude (the data is identical but G assumes $T = 12s$, while H assumes $T = 7s$).

The results are roughly consistent with those of the previous section where the expected Φ_{RMS} for the sum of $\pm$ measurements was calculated using the SSW system noise spectrum.

8.2.3 Amplification

An amplifier ~x30 gain used in some of the measurements did not show a dramatic improvement (Figure 16 and measurements D and E in Figure 15); this amplifier was just upstream of the PDI and apparently noise sources already had affected the signal. Measurements of integral strength at zero current made using a 7-element "Litz" wire (connected in series) *did* reduce noise significantly (Figure 17), and so with early amplification of the signal, the influence of noise can be expected to be reduced. Near full current, the RMS of measurements made with the Litz wire were about the same as those made with the standard wire (i.e. $\sim 2 \times 10^{-4}$). This may be due to limitations in the power supply stability and measurement ($\sim 1 \times 10^{-4}$) or wire oscillations in the Litz wire (some minor modifications would be necessary to tension this much heavier wire comparably).

8.2.4 Summary

The Φ_{RMS} observed is $1.5\mu V - s$ and would seem to stem from electrical noise in the MTF environment (the PDI noise is less than a third of this). For motions of $25mm$ this limits the RMS variation of integral strength measurements to $\sim 0.003T$. Amplification may be able to reduce the relative influence of noise, allowing integral strength measurements to better than $0.0005T$.

9 Measurements Data

This section presents measurement results of accuracy and repeatability for SSW strength and coordinate measurements of FMI quadrupoles.

9.1 Strength measurement accuracy

The accuracy of the strength measurement relies on accurate measurement of wire motion and induced flux. The stage motion measured by the encoders was checked using an HP laser interferometer system. The target was mounted near the wire support (i.e. $35mm$ above the stage on stage unit 'A' and $50mm$ above the stage on stage unit 'B') and so should include any effects from pitch imperfection in the stages. For the calibration the laser was aligned to the axis of motion to within $\sim 6mrad$ to insure less than 2×10^{-5} error ($0.5\mu m$ over $25mm$) in the measured position caused by $\cos\theta$ effects.

The $\pm$ distances travel by the 'A' and 'B' x-stages, along with the corresponding distances recorded by the linear encoders of the stages are given in Figure 18. Calculating a D_{eff} for the interferometer data (by averaging the $\pm$ averages at both ends) gives $D_{eff} = 24.9990mm$; for the encoder data, $D_{eff} = 24.9985mm$. Therefore, the difference in the D_{eff} used in calculating strength is about $0.5\mu m$ and should give an error in strength of 5×10^{-5} (Eqn. 11). The PDI voltage and linearity were calibrated against an HP3458A and found to be accurate to 5×10^{-5} [3]. The long term stability of these calibrations have not yet been verifed.

Thus the present system accuracy would seem to be on the order of $1 - 2 \times 10^{-4}$ (see Section 5.2) assuming accurate measurement of magnet current and removal of multipole effects.

9.2 Strength repeatability

Repeatability data taken near full field are shown in Figure 19. Zero current measurements are shown in Figures 16 and 17 for various configurations (see Section 8.2). The variation in integral strength is very typically $\sim 0.003T$. As an example of long term repeatability, results of three measurements of the reference magnet IQC020-0 performed during a six month period (May-November 1995) are shown in Figure 20. The standard deviation among the measurements is $\sim 1.25 \times 10^{-4}$ (the individual means used were each averages of three repetitions).

9.3 x_0 results

The systematic error from disparity in $\pm x$ motion as measured by the interferometer calibration would seem to be $1 - 2\mu m$. Multiple measurements of x_0 at a fixed current are shown in Figure 21 and have standard deviation

$< 1\mu m$. The measured x_0 compared to optical survey of the laminations is shown in Figure 22 for several magnets. The standard deviation is $112\mu m$ (the typical error in survey measurements cited is $125\mu m$).

9.4 y_0 results

An example of 30 y_0' measurements taken at various tensions is shown in Figure 23. The standard error in the intercept, y_0, for these measurements is $< 2\mu m$. Typically, taking three sweeps at each of three tensions, this error is at the level of $5\mu m$.

Measured y_0 compared to optical survey of the laminations is shown in Figure 24 for several magnets. The RMS is $90\mu m$. Typical error in survey measurements is again $\sim 125\mu m$.

9.5 θ_r results

Roll angle measurements have been a lower priority for the FMI quadrupoles, and there is a smaller quantity of data available. Two calibrations of the system roll offset, θ_e, have yielded a value of $-40 \pm 10\mu rad$. SSW measured roll angle compared to optical survey is shown in Figure 25 for five magnets (note that there are two measurements on magnet IQD020 - one made with the magnet leveled and the other with the magnet intentionally rolled by $\sim 1mrad$). Repeated SSW measurements of roll angle on a single magnet are shown in Figure 26 these indicate measurement repeatability with standard deviation $< 10\mu rad$.

10 Conclusion

Details of the design and performance of the SSW system have been presented and indicate that the system performs at or above its design goals. Results would indicate integral quadrupole strength resolution of 0.003T (perhaps as low as $0.0005T$ with amplification), measurement accuracy of 2×10^{-4}, x, y offsets accuracy of $10\mu m$, and roll angle measurement accuracy of better than $100\mu rad$.

Acknowledgements

The contributions of Clark Reid, Ed E. Schmidt, and James Sim to the development of mechanical, electrical, and software components for the SSW system are gratefully acknowledged.

References

[1] G. Knies and J. Krzywinski, *The DESY Stretched Wire System for Magnetic Measurements*, to be published.

[2] J. DiMarco and J. Krzywinski, *Suggestions for a Single Moving Stretched Wire System at MTF*, MTF-95-0012, 1995.

[3] D. Orris, private communication.

[4] J. W. Sim et. al., *Software for a Database-Controlled Measurement System at the Fermilab Magnet Test Facility*, Proceedings of the 1995 IEEE Particle Accelerator Conference.

[5] J. DiMarco, *Quadrupole Strength Measurements at MTF Using a Single Moving Stretched Wire*, MTF-94-0045, 1994.

[6] J. Strait, private communication.

[7] J. Billan, *Materials*, Proceedings of the Cern Accelerator School on Magnetic Measurement and Alignment, 1992.

[8] M. Thompson, *Main Injector Quadrupole Single Stretched Wire Measurement Procedure*, MTF document in preparation.

11 Appendix A - Components

Below is a list of FNAL drawings associated with the SSW system:

Drawing Name	Drawing Number
ISOTHERMIC FLASK-WIRE CONNECTOR	1670-MA-304621
DRIVE MOTOR-PULLEY	1670-MA-304620
SPHERICAL PAD-MOUNTING PLATES	1670-MC-304614
STRAIN RELIEF-MOUNTING BLOCK	1670-MA-304613
SUPPORT TABLE-BASE PLATE	1670-MC-304612
STAGE SUPPORT TABLE	1670-MD-304611
ADJUSTMENT PLATE(DOUBLE SHAFT)	1670-MC-304610
ADJUSTMENT PLATE(SINGLE SHAFT)	1670-MC-304609
WIRE POSITIONER SUB-ASSEMBLIES	1670-MC-304606
PLATE MODIFICATIONS(TENSION END)	1670-MC-304605
PLATE MODIFICATIONS(MOTOR END)	1670-MC-304604
JEWEL	1670-MA-304602
JEWEL HOLDER-MOUNTING BRACKETS	1670-MB-304601
JEWEL HOLDER/CLAMP-TYPE 2	1670-MC-304594
JEWEL HOLDER/CLAMP-TYPE 1	1670-MC-304593

Below is a partial listing of components:

Component Name	Model	Vendor
Stages	SL202	Pacific Precision Labs (PPL)
Heidenhain encoders	1um accuracy	PPL
Home, limit switches	10um	PPL
Microlevel	5urad	Wyler
Step motor translators	SMD	Whedco
Controllers	VME-3560	Whedco
Precision Digital Integrator	5035	Metrolab
Ceramic wire guides	-	Keir Ceramics
Tension Gauge	0.5-mini-utc	A. L. Design Inc.
Flasks	H19876, F19860	Southeastern Lab. Apparatus
Retro-reflector nest	1.5 SM	Hubbs Machine and Manufacturing
Step motor (for wire tension)	LN-5751	Compumotor/Parker
CuBe wire	#25 alloy 100um	Little Falls Alloy

12 Appendix B - Effects of Offset and Motion Error

Taking a thin cross-sectional slice of the wire of length dz at an axial position z, the flux measured in moving the wire from initial position $x_0(z)+\epsilon_{0_+}$ to final position $D + x_0(z) + \epsilon_+$ (from Eqn. 1) is

$$\Phi_{H+}(z) = dz \int_{x=\epsilon_{0_+}}^{D+\epsilon_+} g\,(\,x - x_0(z)\,)\;dx$$

where the ϵ's are small offsets from desired start and stop positions as measured by the encoders (i.e. the stages are requested to start at position 0 and move a distance D, but depending on whether stages are operating with feedback , etc., the stages start and stop a small amount off the requested values). The x_0 is left as a function of $z-$position since the stretched wire axis may not be set up parallel to the magnet axis.

$$\begin{aligned}\Phi_{H+}(z) &= dz\, g \left(\frac{x^2}{2} - x_0(z)x \right)\Bigg|_{\epsilon_{0_+}}^{D+\epsilon_+} \\ &\approx dz\, g \left(\frac{D^2 + 2D\epsilon_+}{2} - x_0(z)D - x_0(z)\epsilon_+ + x_0(z)\epsilon_{0_+} \right)\end{aligned}$$

Similarly for the move in the $-D$ direction (from initial position $x_0(z)+\epsilon_{0_-}$ to final position $-D + x_0(z) + \epsilon_-$)

$$\Phi_{H-}(z) \approx dz\, g \left(\frac{D^2 - 2D\epsilon_-}{2} + x_0(z)D - x_0(z)\epsilon_- + x_0(z)\epsilon_{0_-} \right)$$

12.1 Strength

Combining $\Phi_{H+}(z) + \Phi_{H-}(z)$ for measurement of strength yields

$$\begin{aligned}\Phi_{H+}(z) + \Phi_{H-}(z) &= dz\, g \left[D^2 + D(\epsilon_+ - \epsilon_-) - x_0(z)(\epsilon_+ + \epsilon_-) + \right. \\ &\qquad \left. x_0(z)(\epsilon_{0_+} + \epsilon_{0_-}) \right]\end{aligned}$$

For $D \sim 25mm$, ϵ's $\sim 5\mu m$, $x_0(z) \sim 2.5mm$, the $x_0(z)\epsilon$ terms amount to a few $\times 10^{-5}$ of D^2 and can be ignored. We are left with

$$\Phi_{H+}(z) + \Phi_{H-}(z) = dz\, g \left[D^2 + D(\epsilon_+ - \epsilon_-) \right] \qquad (35)$$

Alternatively, taking a D_{eff} as the average of encoder values at the extremum positions gives

$$\begin{aligned} D_{eff} &= \frac{(D+\epsilon_+)-(-D+\epsilon_-)}{2} \\ &= D+\frac{\epsilon_+-\epsilon_-}{2} \end{aligned}$$

From Eqn. 3 this gives

$$\begin{aligned} \Phi_{H+}(z)+\Phi_{H-}(z) &= dz\, g\, D_{eff}^2 \\ &\approx dz\, g\, \left(D^2+D(\epsilon_+-\epsilon_-)\right) \end{aligned}$$

which is the same as the flux sum of Eqn. 35 above. Note that this result is independent of x_0 (and hence on z) - depending neither on the offset nor on the wire being parallel to the magnet axis. Therefore, over the axial integration in z, dz is replaced by L_m, the magnetic length, and ϵ_+ (or ϵ_-) by the average ϵ_+ (ϵ_-)of the two ends of the wire; simply averaging the $\pm$ extrema positions reported by the encoders at both ends of the wire (and ignoring those at the zero positions) gives a very accurate measure of D_{eff}.

12.2 Centering

The effect of the offsets (ϵ's) on determining centering parameters is found by calculating x_0' with $\Phi_{H\pm}$ as above. This yields

$$x_0' = x_0(z)-(\epsilon_+ + \epsilon_-)+\frac{x_0(z)}{2D}((\epsilon_+-\epsilon_-)-(\epsilon_{0_+}-\epsilon_{0_-}))$$

For the sample parameters given above, $\frac{x_0(z)}{2D} \approx 0.05$ which, when multiplied by a quantity of order ϵ can be ignored. This leaves

$$x_0' = x_0(z)-(\epsilon_+ + \epsilon_-)$$

This shows that offsets in the motion extrema get carried directly to an error in determined position. If encoders record these offsets accurately, they can be corrected for, but if there are no encoders or errors in encoder reading, or if the offsets stem from stage errors or wire motion on the jewels, the consequent errors will carry through.

13 Appendix C - Additional Measurements

13.1 Quadrupole axis determination

Previously we considered the wire to be at position $x - x_0$, $y - y_0$ with respect to the magnet axis (where x, y is the position in the SSW frame and x_0, y_0 is the translation offset between the SSW and magnet frames). If however, one end of the wire is translated by a different amount than the other end, the unequal displacement raises the question of what the center offsets calculated by the SSW measurements mean. Considering a wire of length L (from $z = 0$ to $z = L$) and a magnet the ends of which are located at $z = a$, $z = b$, the position of the wire at any point in the magnet is given by

$$\begin{aligned} x_m &= x - \frac{x_b - x_a}{b - a}(z - a) - x_a \\ y_m &= y - \frac{y_b - y_a}{b - a}(z - a) - y_a \end{aligned}$$

where the x_b, x_a, y_b, y_a are the x, y offsets of the wire at the $z = b$, $z = a$ ends of the magnet. If we use this in Eqn. 1, we have

$$\Phi_{H\pm} = \int_{z=a}^{b} \int_{x=0}^{\pm D} g\,[b_2\, x_m - a_2 y_m]\, dx$$

This yields

$$\Phi_{H\pm} = gL_m \left[b_2 \frac{D^2}{2} \mp D \left(x_a b_2 + a_2 y - a_2 y_a + \frac{b_2}{2}(x_b - x_a) - \frac{a_2}{2}(y_b - y_a) \right) \right]$$

Determining x_0' from Eqn. 5 then gives

$$x_0' = \frac{x_b + x_a}{2} \tag{36}$$

i.e. the offset determined is simply the average offset (note, however, that if the distances $z = 0$ to $z = a$ or $z = b$ to $z = L$ are large and $x_a \neq x_b$, then transfer errors (from the stages to magnet fiducials) can result because the position of the wire at the stages is different than its position at the ends of the magnet (see Section 7)). This average offset is appropriate to use in transfer to magnet fiducials and subsequently in component alignment.

If the wire ends are moved counter-directionally (i.e. one stage moving from 0 to $x = D$ while the other moves from 0 to $x = -D$), the result can be combined with the above to determine the axis of the magnet ([6]). For counter-directional stage motion the flux is evaluated as before except that x (in the wire's frame) is now a function of z and thus the limits for x integration must go from $x = 0$ to $x = \pm D\left(1 - \frac{2z}{L}\right)$. Peforming the integration yields

$$\begin{aligned}\Phi_{H\pm} &= \int_{z=a}^{b}\int_{x=0}^{\pm D\left(1-\frac{2z}{L}\right)} g\left[b_2\, x_m - a_2 y_m\right] dx \\ &= gL_m\left[b_2\frac{D^2}{2}\alpha_3 \mp D\left(x_a b_2\alpha_2 + a_2 y\alpha_2 - a_2 y_a\alpha_2 + \right.\right. \\ &\qquad \left.\left. -b_2(x_b - x_a)\alpha_2 + a_2(y_b - y_a)\alpha_2\right)\right]\end{aligned}$$

where the α's are the geometrical factors

$$\begin{aligned}\alpha_1 &= 1 - \frac{b+a}{L} \\ \alpha_2 &= \frac{2a+4b-3L}{6L} \\ \alpha_3 &= 1 - \frac{2(b+a)}{L} + \frac{4}{3}\frac{a^2+b^2+ab}{L^2}\end{aligned}$$

For small roll angle, the a_2 terms can be ignored and calculation of x_0' from Eqn. 5 gives

$$x_0' = x_a\frac{\alpha_1+\alpha_2}{\alpha_3} - x_b\frac{\alpha_2}{\alpha_3} \tag{37}$$

Therefore, with measurement of x_0' using co-directional and counter-directional stage motions, Eqns. 36 and 37, can be used to determine the values of the two unknown quantities, x_a, x_b, relative to the wire position at the ends of the magnet.

A similar set of measurements can be made to yield the y_a, y_b except with additional efforts needed to remove sag influences using $1/T$ extrapolations to infinite tension.

13.2 Dipole magnet strength

For a stretched wire measurement in a dipole magnet, where the general expression for the $y-$component of the field is given by

$$B_y = B_1 \sum_{n=1}^{\infty} (\frac{1}{R})^{n-1} \left[b_n \Re\{((x-x_0)+i(y-y_0))^{n-1}\} - a_n \Im\{((x-x_0)+i(y-y_0))^{n-1}\}\right]$$

the integral strength, $L_m B_1$, can be determined from the flux measured for horizontal wire motion

$$\begin{aligned}
\Phi_H^{\pm}(y) &= \int dz \int_0^{\pm D} dx B_y(x,y) \\
&= \Phi_H^{\pm} = L_m B_1 x \left(b_1 + \frac{b_2}{2}\left(\frac{x}{R} - \frac{2x_0}{R}\right) - \frac{a_2}{2}\left(\frac{2y}{R} - \frac{2y_0}{R}\right)\right. \\
&\quad + \frac{b_3}{3}\left(\frac{x^2}{R^2} + \frac{3x_0^2}{R^2} - \frac{3y_0^2}{R^2} - \frac{3x_0 x}{R^2} + \frac{6yy_0}{R^2} - \frac{3y^2}{R^2}\right) \\
&\quad \left. + \frac{a_3}{3}\left(\frac{-6x_0y_0}{R^2} + \frac{3y_0x}{R^2} + \frac{6x_0y}{R^2} - \frac{3xy}{R^2}\right) + \ldots\right) \Big|_0^{x=\pm D}
\end{aligned}$$

Taking the difference of $\pm$ measurements at $y = 0$ leaves

$$\begin{aligned}
\frac{\Phi^+ - \Phi^-}{2} &= L_m B_1 D \left(b_1 + \frac{-b_2}{2}\left(\frac{2x_0}{R}\right) - \frac{a_2}{2}\left(-\frac{2y_0}{R}\right)\right. \\
&\quad + \frac{b_3}{3}\left(\frac{D^2}{R^2} + \frac{3x_0^2}{R^2} - \frac{3y_0^2}{R^2}\right) \\
&\quad \left. + \frac{a_3}{3}\left(\frac{6x_0y_0}{R^2}\right) + \ldots\right)
\end{aligned}$$

where the first term, $L_m B_1 D b_1$, yields the integrated strength. The multipole terms are generally small and can be neglected (or removed in analysis as needed). For example, $R = 0.0254m$, x_0, $y_0 < 5mm$ and wire motion is $D = \pm 10mm$, the dominant error from multipoles is $\sim 0.2 \times b_2$. Errors arising from the measurement of flux for this same motion (assuming $L_m = 3m$, $B_1 \sim 1.5T$, and RMS flux error $\sim 2\mu V - s$) would cause errors in the measured strength $\sim 0.5 \times 10^{-4}$ and so are likewise generally small. In addition to centering the wire in x, y to better than $5mm$, the result would also depend on adjustment of the the roll angle, $b_1 = \cos\theta_1$, to within $15mrad$ for errors less than 10^{-4}.

13.3 Dipole magnet field shape

If SSW measurements are made at several motion steps, e.g. $D = 10mm$, $15mm$, $20mm$, etc., the change in field as a function of x can be measured from the differences between successive $\Phi_H^{\pm}$. It is therefore also possible to roughly determine the multipole strengths. For example, using the expression for Φ_H^+ in the previous section, setting $y = y_0 = 0$, and defining the difference between successive wire motions as $w = D_{i+1} - D_i$,

$$\Phi_H^+\Big|_0^{D_i+w} - \Phi_H^+\Big|_0^{D_i} = L_m B_1 w \left(b_1 + b_2 \left(\frac{(D-x_0)}{R} + \frac{w}{2R} \right) + b_3 \left(\frac{(D-x_0)^2}{R^2} + \frac{(D-x_0)}{R^2} w + \frac{w^2}{3R^2} \right) + \ldots \right)$$

This is an expression for the flux through a loop of width w at position $D - x_0$, and the variation as a function of D can thus be mapped. Furthermore, to first order, the term linear in D is $\frac{b_2}{R}$, and the term quadratic in D is $\frac{b_3}{R^2}$, etc., and determining the coefficients of a polynomial fit of this data directly gives an estimate of the multipoles (because of the fitting involved, care must be taken in estimating the uncertainty in the multipoles measured - especially higher order terms).

13.4 Dipole magnets with sagitta

For dipole magnets with sagitta, the position of the magnet axis relative to the SSW system is a function of axial position, z. This is given by

$$\begin{aligned} x_0(z) &= r - r\cos\theta + x_0(0) \\ &= r - r(\sqrt{1-\sin\theta^2}) + x_0(0) \\ &= r(1 - \sqrt{1 - \frac{z^2}{r^2}}) + x_0(0) \\ &= \frac{z^2}{d} + x_0(0) \end{aligned}$$

where $r = \frac{d}{2}$ is the radius of curvature of the magnet and $z = 0$ is taken to be magnet center with the ends at $\pm L_m/2$.

The result of the flux calculation is the same as for straight dipoles except that there are additional contributions from multipole terms. The dominant terms, assuming that x_0, y_0 are $< R/10$ and that the strength is calculated

from $(\Phi^+ - \Phi^-)/2$, are

$$\frac{b_2}{12}\frac{L_m^2}{dR} + \frac{b_3}{3}\frac{D^2}{R^2} + \frac{b_3}{80}\left(\frac{L_m^2}{dR}\right)^2 + \ldots$$

For the FMI dipoles $L_m = 6m$, $d = 2340m$, and $R = 0.0254$ so that for $D = 0.01m$, the largest contribution to error would be $\sim 0.05b_3$.

14 Appendix D - Susceptibility and Sag Effects

14.1 Wire sag

The weight of a wire causes it to sag a distance Δy equal to

$$\begin{aligned} \Delta y &= c\,(cosh\frac{z}{c} - 1) \\ &\approx \frac{z^2}{2c} \end{aligned}$$

where z is the axial position of the end of the wire from center, and $c = T/w$ (T is the horizontal tension in the wire, and the w is the weight per unit length).

CuBe wire has density $\sim 8.4 \times 10^3 \frac{kg}{m^3}$ and tensile strength $\sim 1400MPa$. This gives a value of $c =\sim 17km$ (assuming T is near its tensile limit) and therefore at $z = L_m/2 = 1.5m$, a sag of $\Delta y = 70\mu m$. Note that the average displacement ($\sim 2/3$ this amount) is what actually would be measured.

For tungsten wire, the density is about $15 \times 10^3 \frac{kg}{m^3}$ and the tensile strength $\sim 2800MPa$. This gives a similar value, $c =\sim 20km$, and so at $z = 1.5m$, $\Delta y = 60\mu m$.

14.2 Wire susceptibility

Following the discussion in [7], the force per unit length in the $x-$direction caused by the wire being dia- or para-magnetic is

$$f = \frac{\chi}{\mu_0} g^2 a x$$

where χ is the susceptibility (of order 10^{-5}), g is the gradient ($\sim 23T/m$ for FMI), x is the $x-$position of the wire in the field ($0.025m$), a is the cross-sectional area of the wire ($8 \times 10^{-9}m^2$ for the $100\mu m$ wire used), and μ_0 is $4\pi \times 10^{-7}\frac{Tm}{A}$. Using these values, $f = 8 \times 10^{-7}\frac{N}{m}$.

For a wire the same length as the magnet, f plays the same role as gravity in a catenary (see above wire sag discussion). The displacement at the center position, $z = L_m/2$, for a wire with the above parameters and T, the wire tension, at $850g$ $(8N)$, is

$$\begin{aligned} \Delta x &= \frac{fL_m^2}{8T} \\ &= 0.1\mu m \end{aligned}$$

and so is negligible for FMI measurements.

If the wire is much longer than the magnet $L_w >> L_m$, the situation approaches that of a wire being pulled at its center point by a localized force equal to fL_m. The displacement in such a case would be

$$\Delta x = \frac{fL_wL_m}{2T}$$

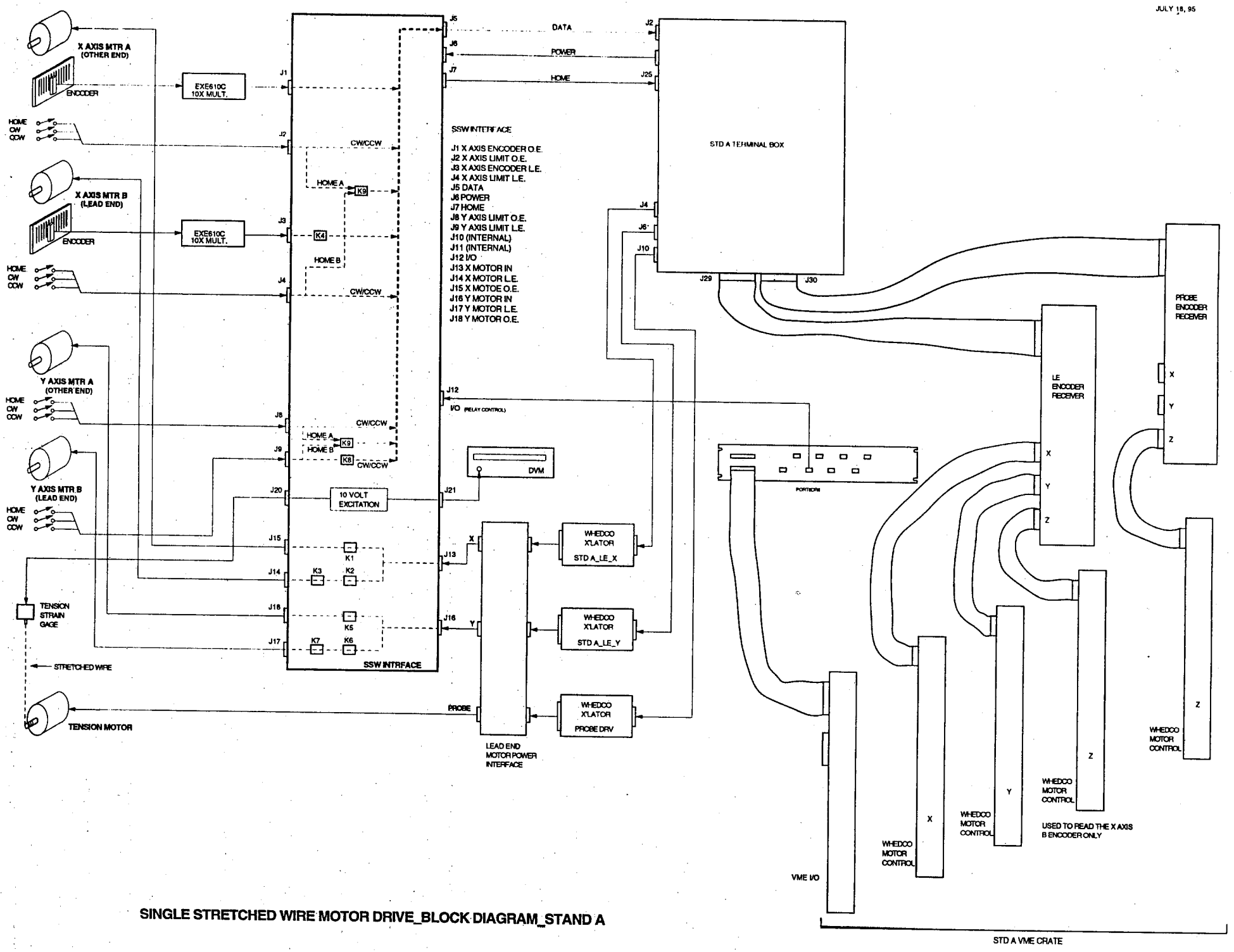

SINGLE STRETCHED WIRE MOTOR DRIVE_BLOCK DIAGRAM_STAND A

Figure 1: Electrical schematic

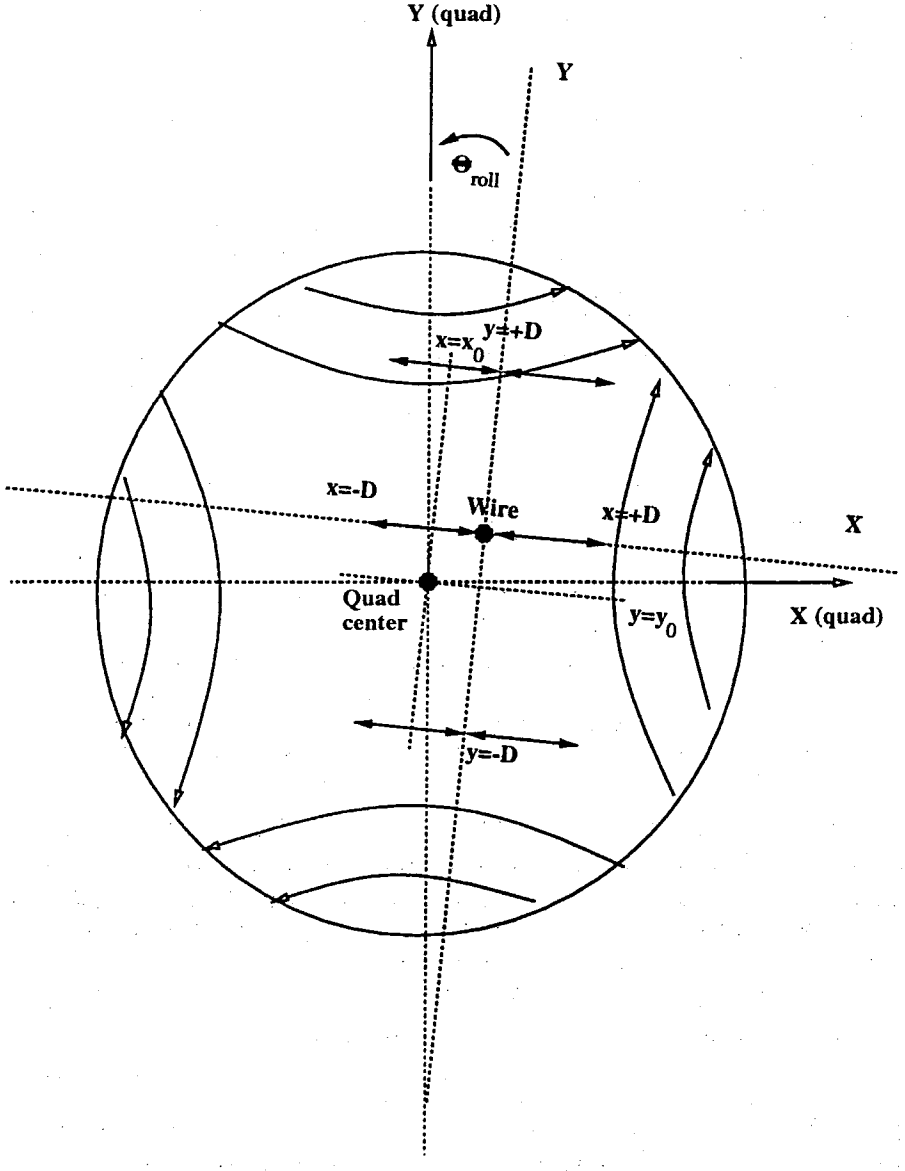

Figure 2: SSW coordinates and motions with respect to magnet

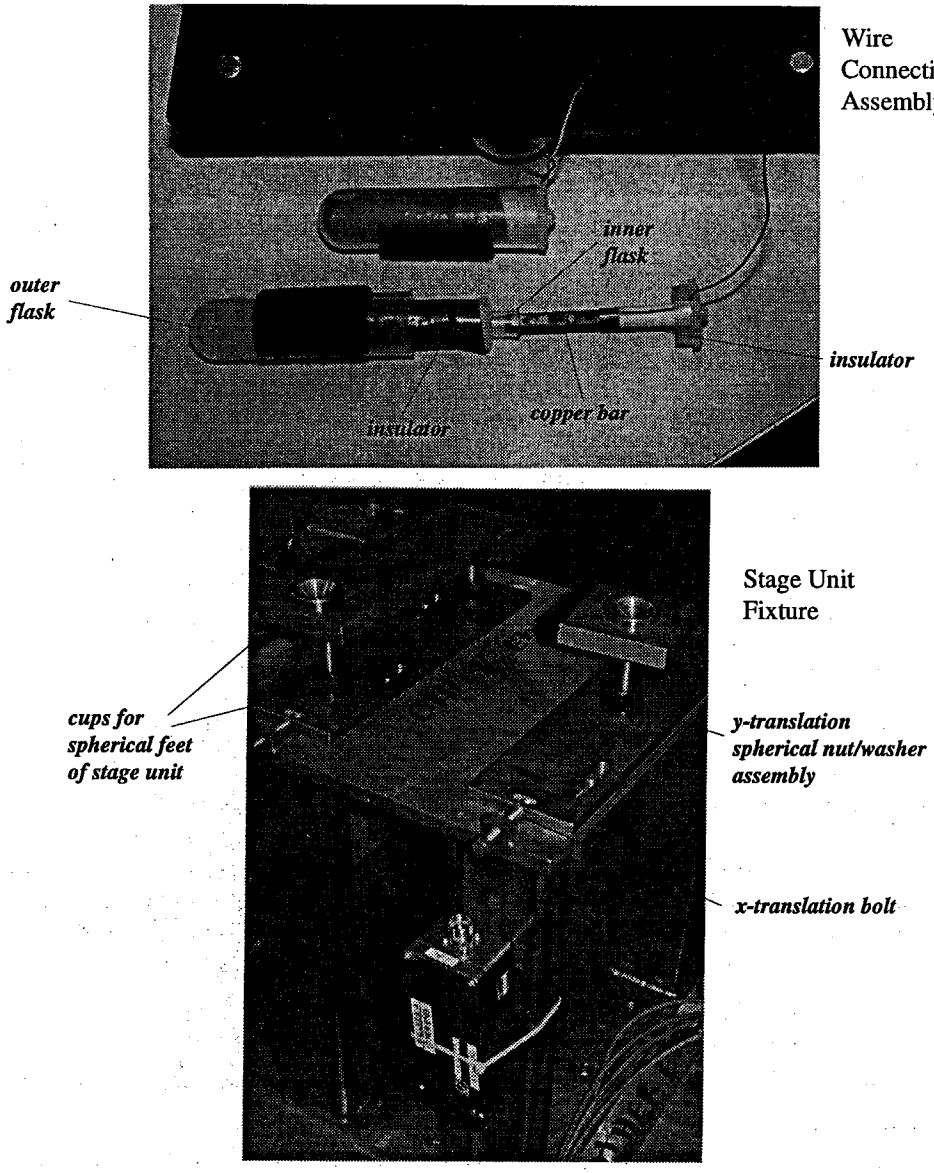

Figure 3: Thermal isolation and stage unit support fixture

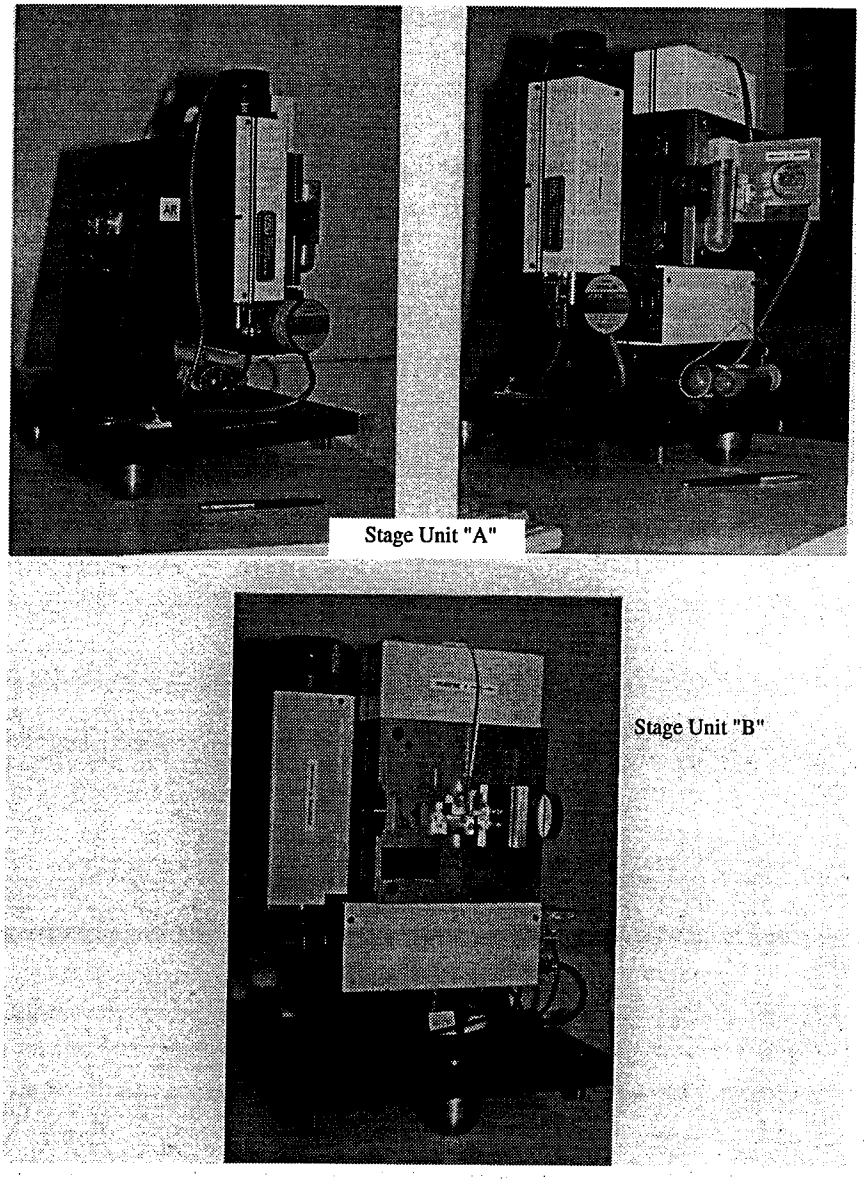

Figure 4: SSW stage units

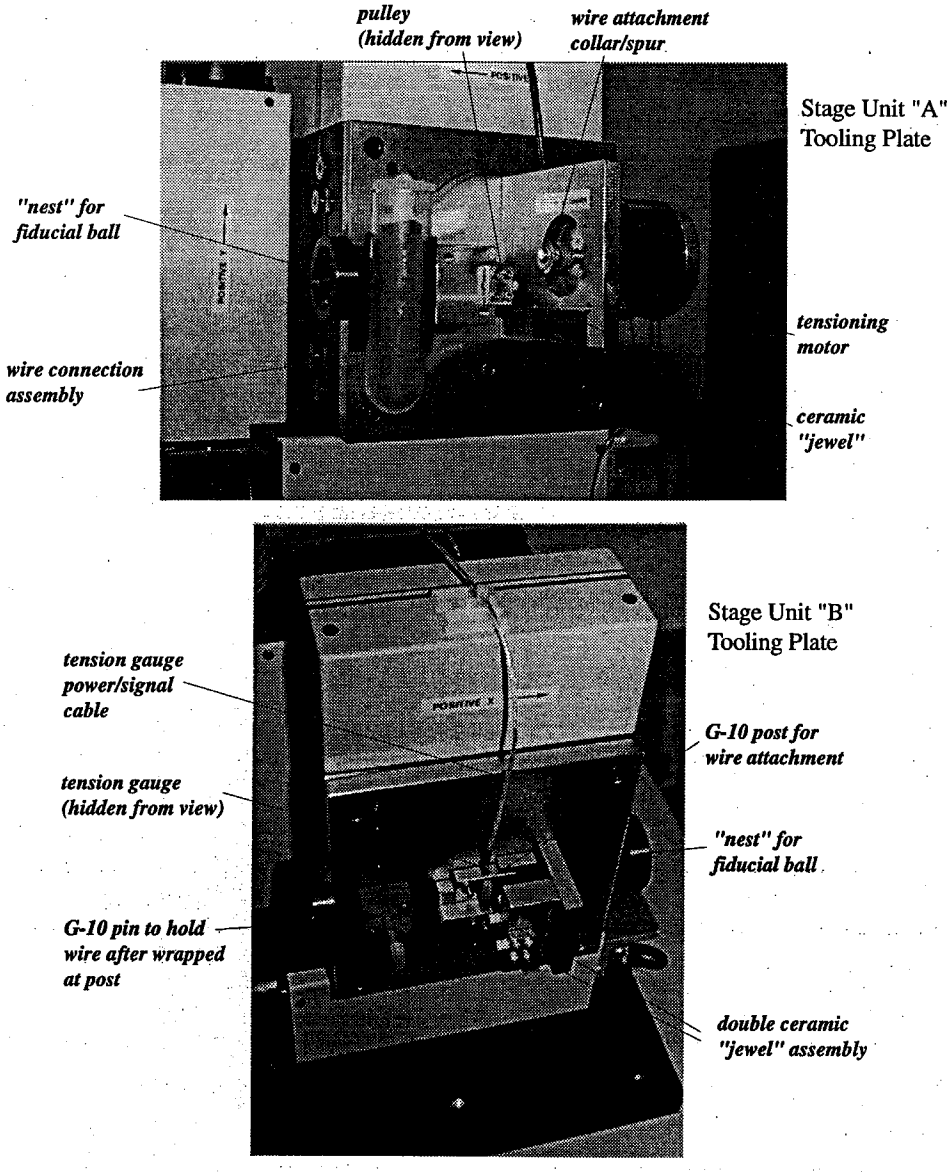

Figure 5: Stage unit wire support and tensioning

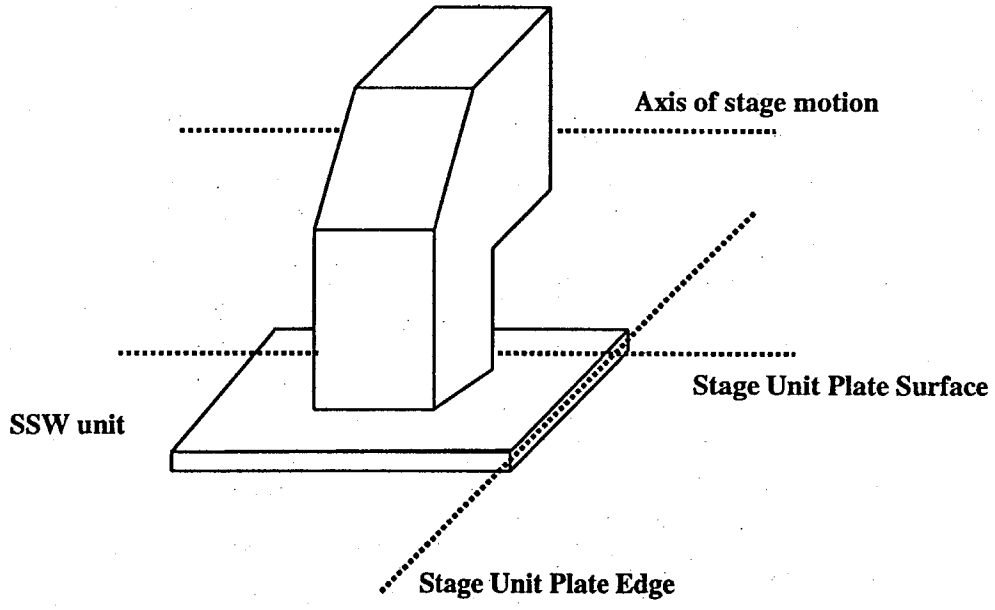

Figure 6: Stage unit plate axes used for alignment

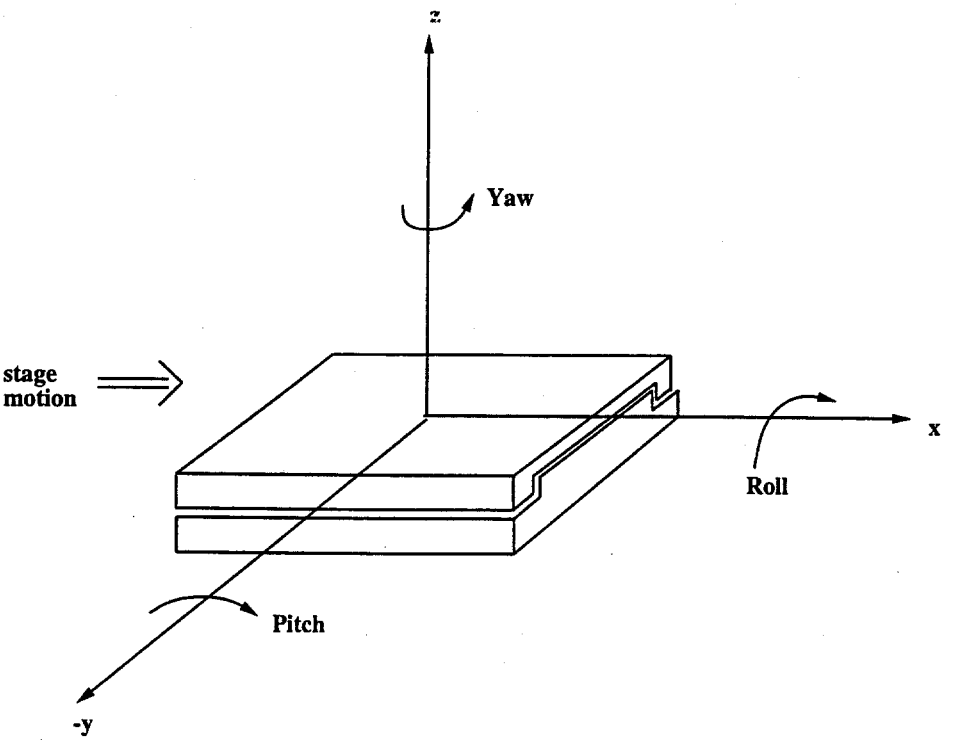

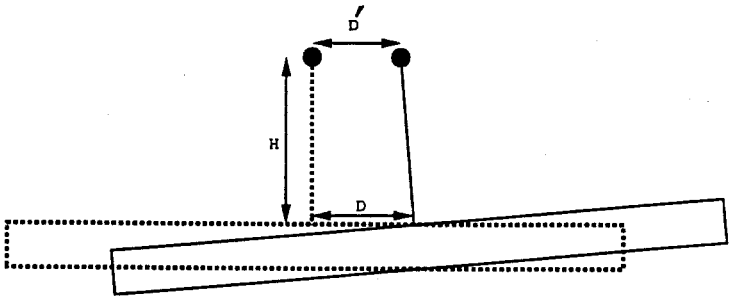

$$D' = D - H \sin \theta_{pitch}$$

Figure 7: Stage axes and error in x-motion caused by pitch error

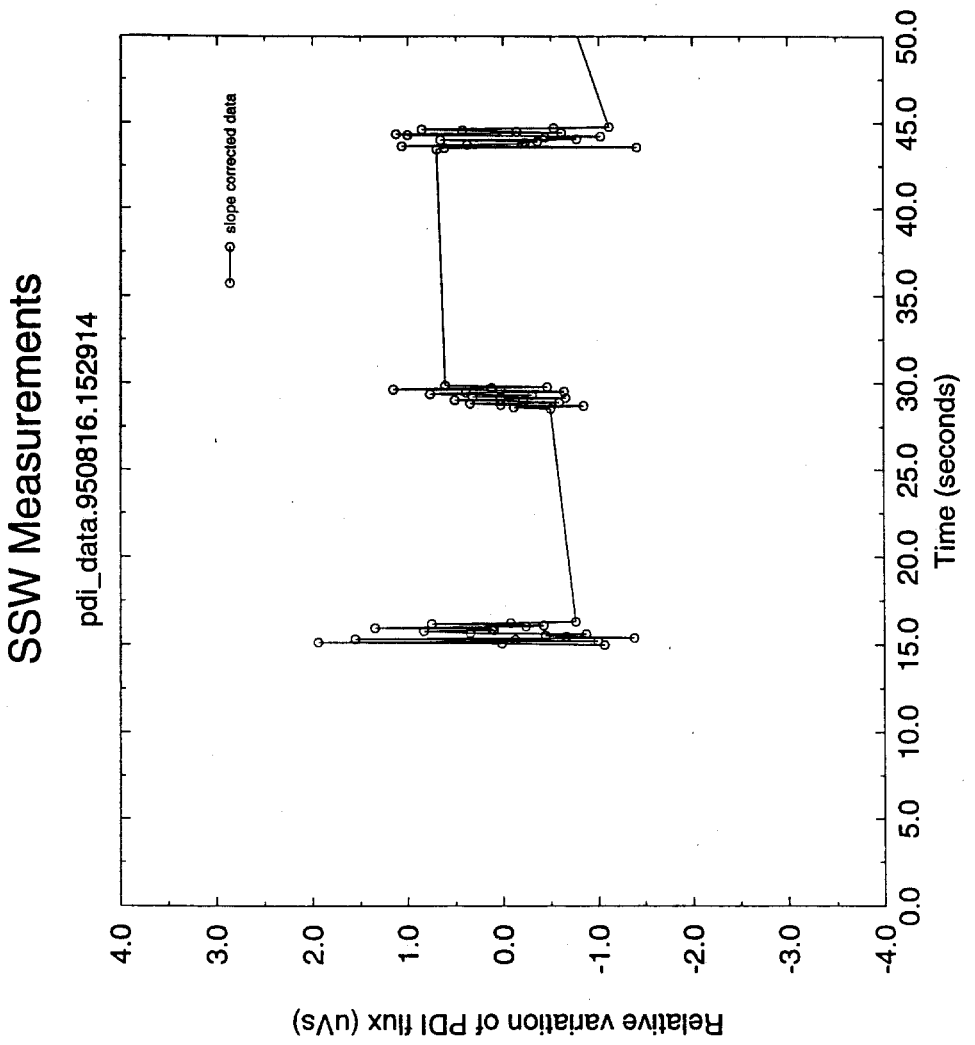

Figure 8: Variations in measured flux with wire "stationary" at extrema of motion

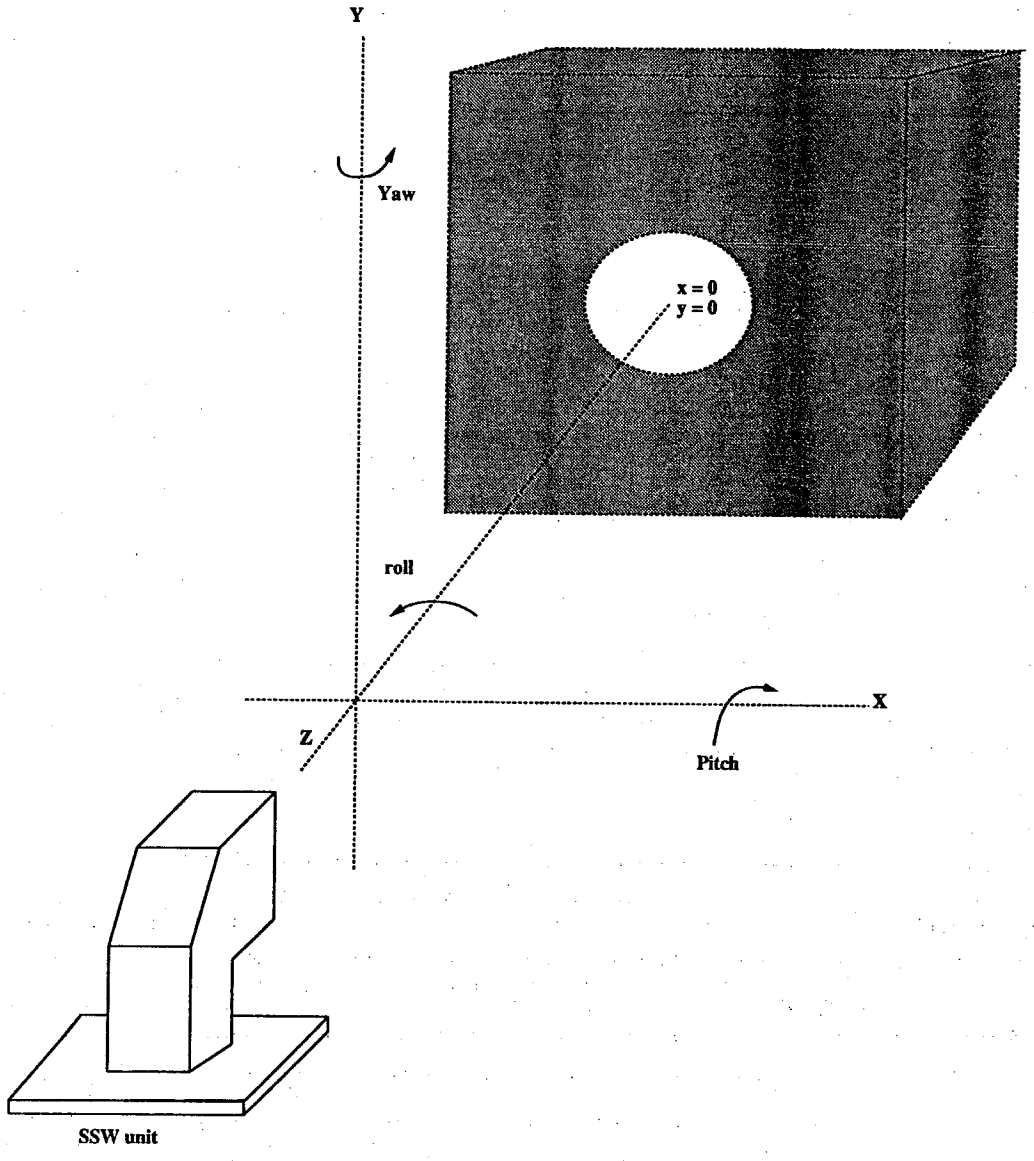

Figure 9: Axes of SSW stage unit

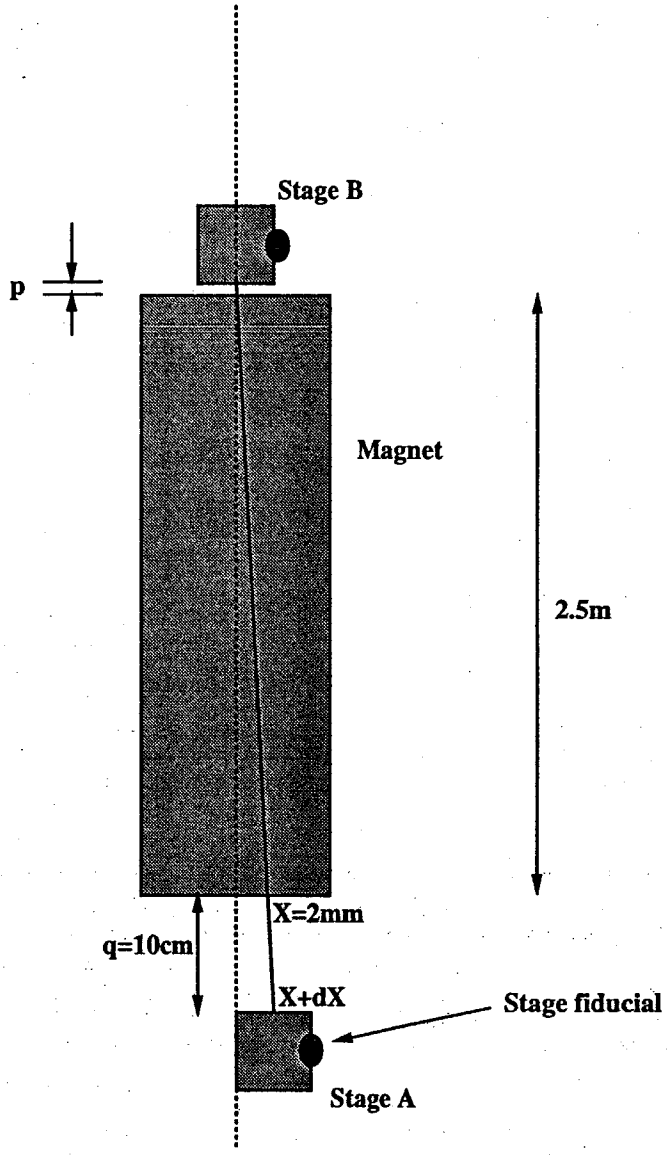

Figure 10: Influence of stage unit positioning at ends of magnet on determination of quadrupole center

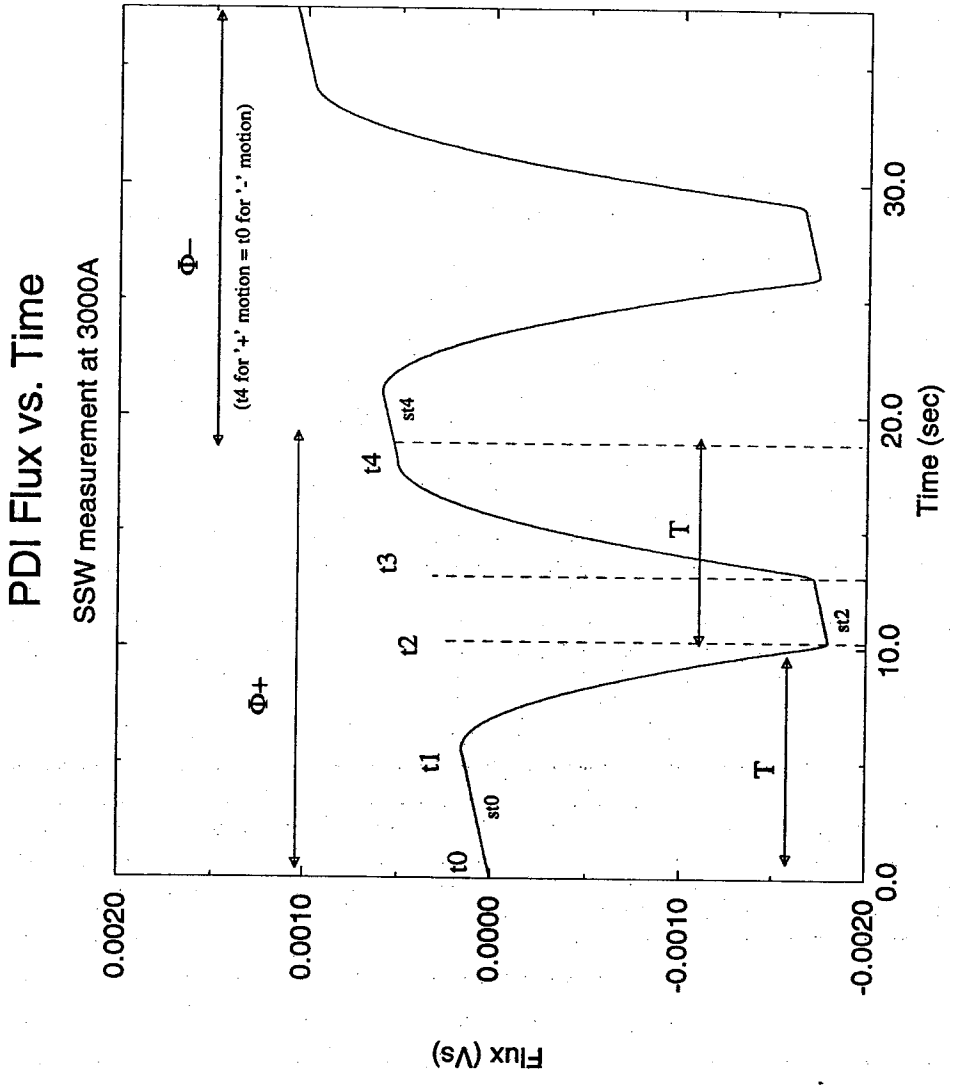

Figure 11: Flux vs Time for a 'typical' SSW measurement scan

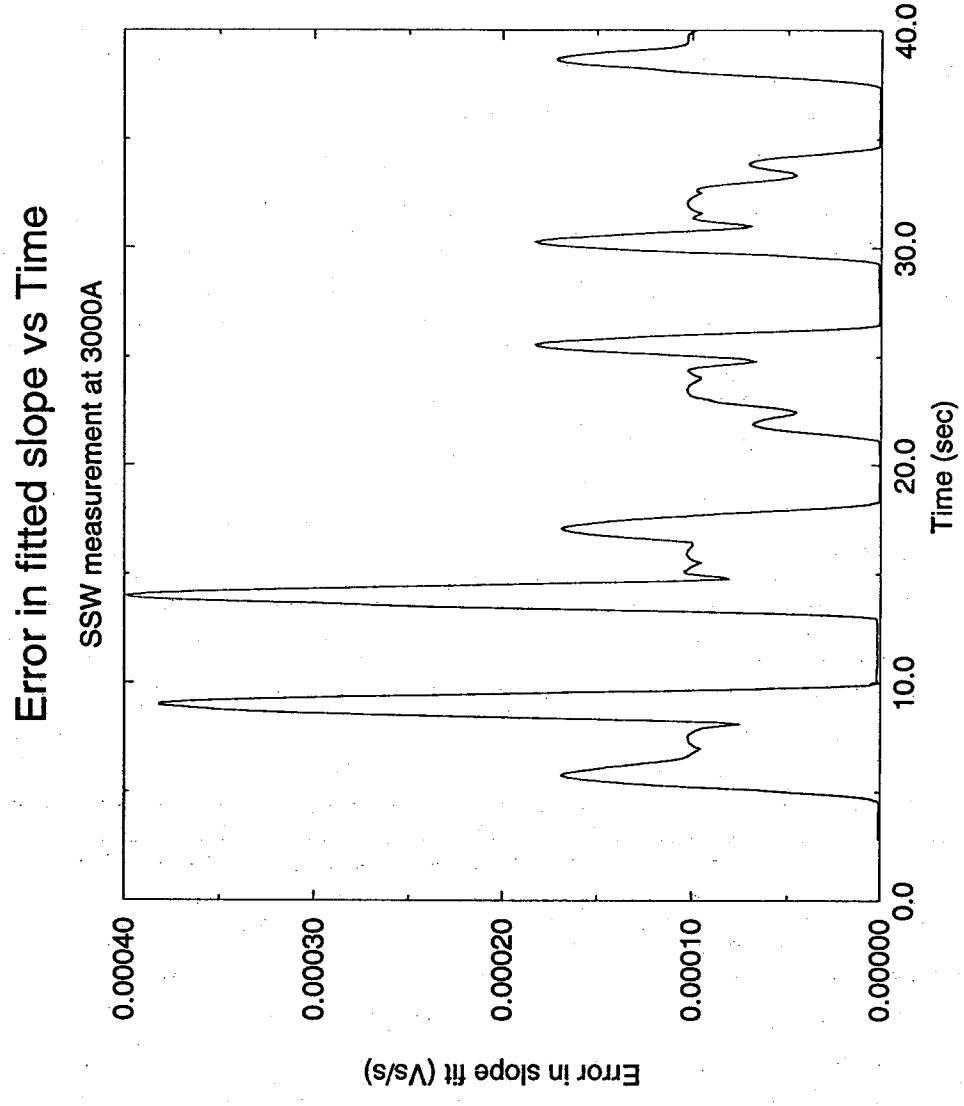

Figure 12: Error of fit vs time for a fixed number of points. Flattops are determined from the minima

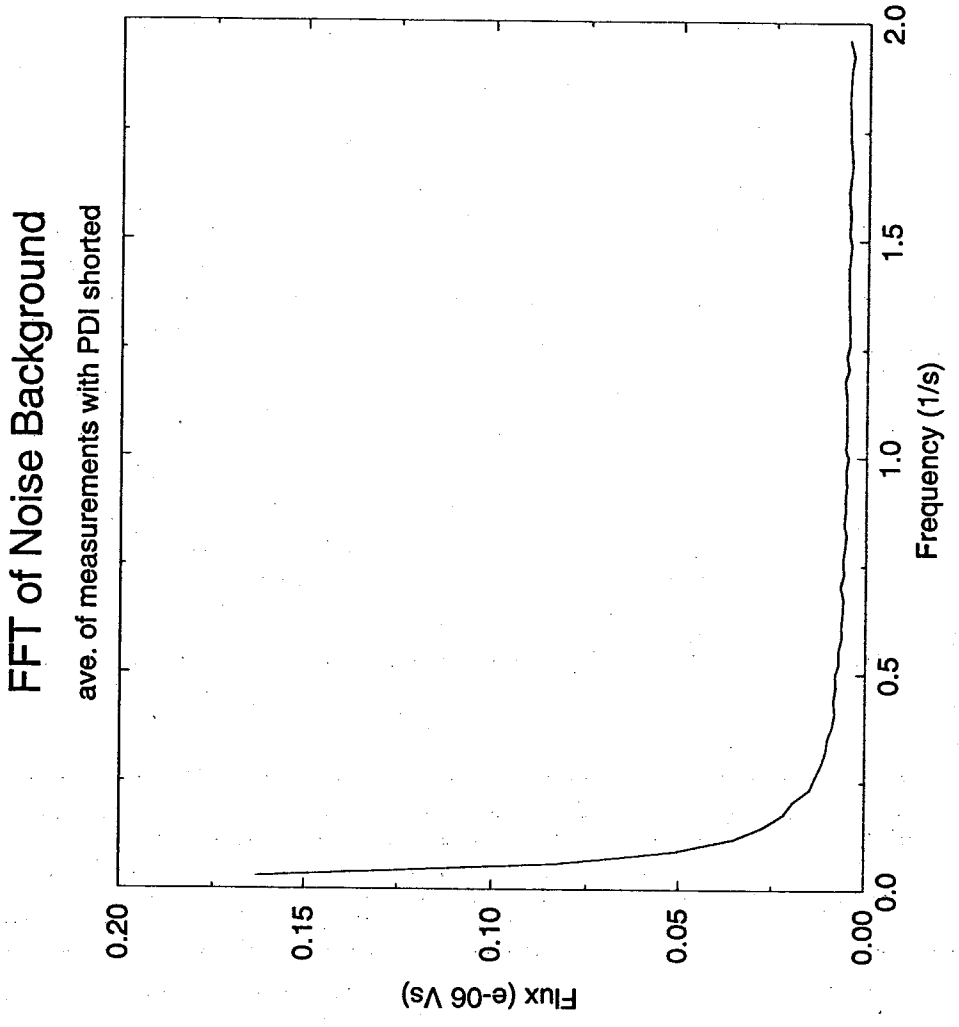

Figure 13: Spectrum of noise with PDI shorted

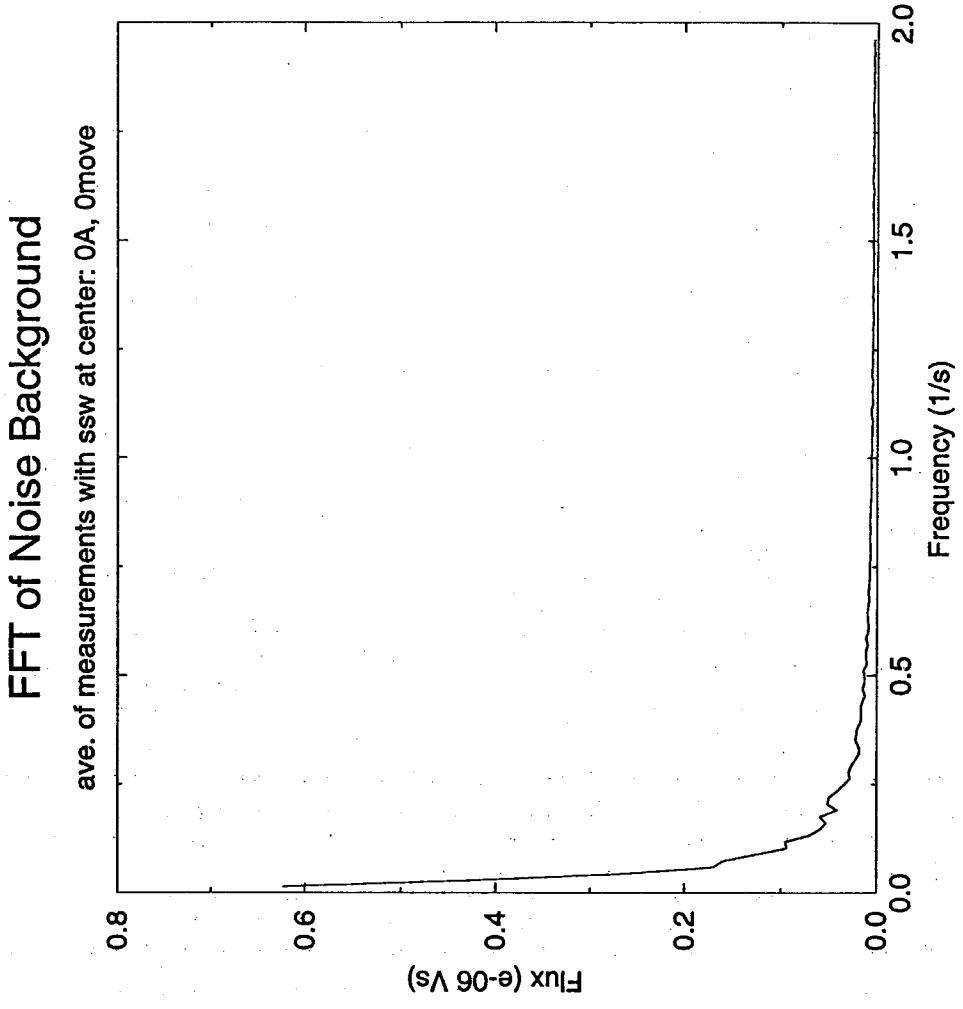

Figure 14: Spectrum of noise with wire attached in low field region at 0A

Total flux (sum of "+" and "-" movement flux) is calculated as if the following noise data were measurement data with flattops separated by T=12s. The RMS of this total flux serves as an estimate of noise contribution to a measurement

	Conditions	time stamp	n	RMS (Vs)
A)	pdi input shorted	950914.102400	50	6.44e-07
B)	ssw 0A, 0 move, low field	950913.152000	20	1.46e-06
		950908.093800	10	1.46e-06
C)	ssw 0A, 12.5mm move	950914.084500	30	2.53e-06
D)	ssw 0A, 25mm move	950913.113500	50	1.90e-06
E)	ssw 0A, 25mm move, 30x preamp	950914.112500	50	1.38e-06
F)	ssw 0A, 25mm move, 30x preamp better thermal stability	950915.150500	50	1.30e-06
G)	ssw 3000A, 0 move, high field pdi input gain x500	950914.164000	20	1.72e-06
H)	ssw 3000A, 0 move, high field flattop sep. 7.0s	950914.164000	20	1.13e-06
I)	ssw 3000A, 25mm move, pdi input gain x500	950914.135000	50	2.44e-06
J)	ssw 3000A, 25mm move, 30x preamp, pdi x10	950914.123500	20	1.81e-06

Figure 15: Summary of noise study measurements

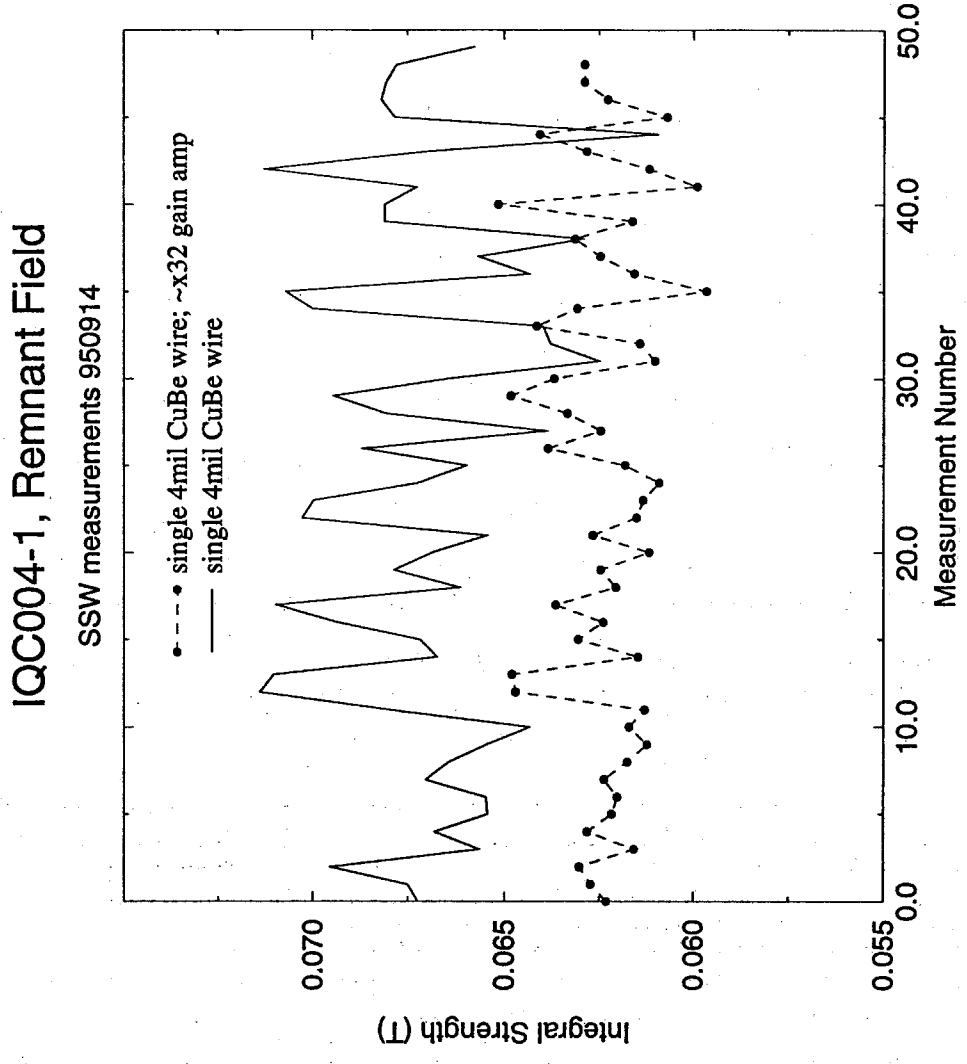

Figure 16: Repeatability measurements at 0A with and without pre-PDI amplifier

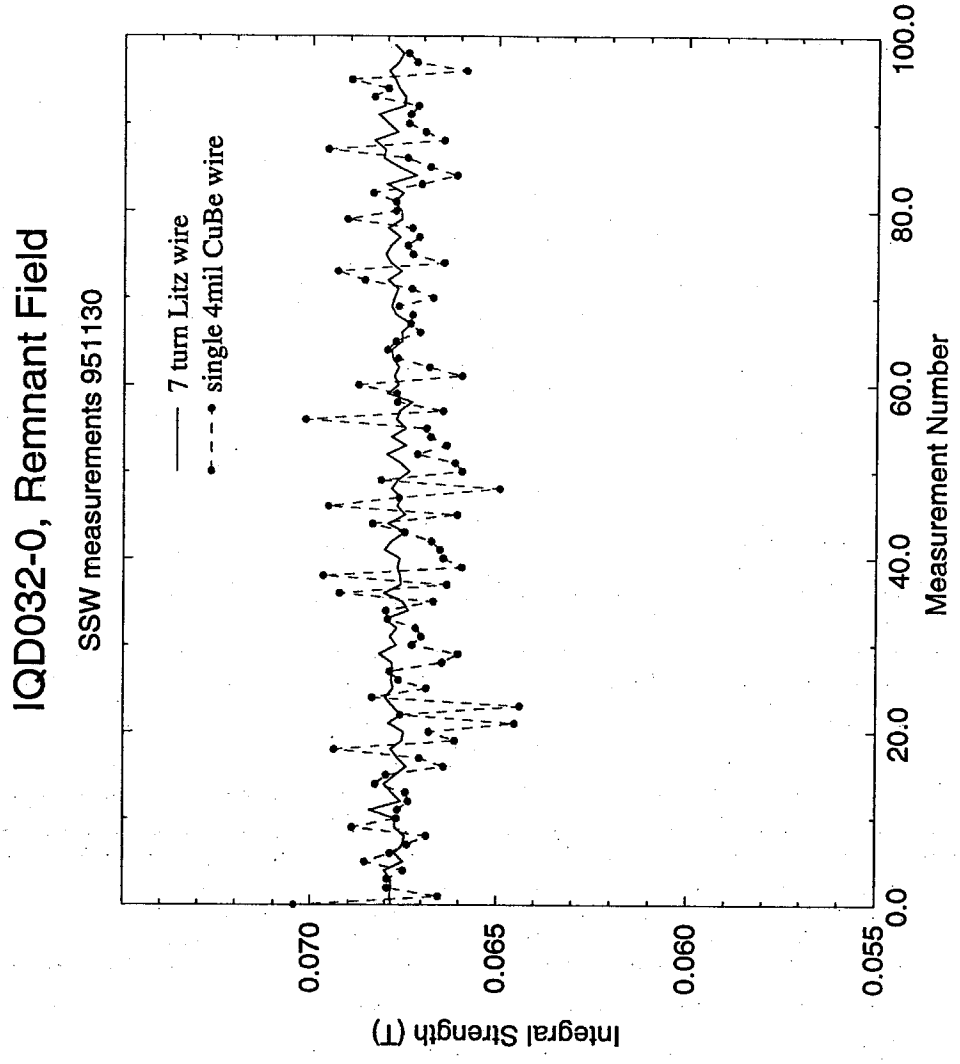

Figure 17: Repeatability measurements at 0A with CuBe and Litz wire

Stage Unit A

n	intf 0	intf -	intf 0	intf +	enc -	enc +
1	0.0006	-24.9988	-0.0018	25.0007	-24.9985	24.9985
2	0.0002	-24.9991	-0.0024	25.0000	-24.9975	24.9985
3	-0.0004	-24.9995	-0.0026	24.9998	-24.9975	24.9985
4	-0.0010	-25.0008	-0.0028	24.9990	-24.9985	24.9985
5	-0.0012	-25.0009	-0.0031	24.9989	-24.9975	24.9985
6	-0.0005	-25.0010	-0.0033	24.9986	-24.9985	24.9985
7	-0.0013	-25.0013	-0.0035	24.9984	-24.9985	24.9985
8	-0.0016	-25.0015	-0.0036	24.9983	-24.9985	24.9985
9	-0.0018	-25.0017	-0.0035	24.9981	-24.9985	24.9985
10	-0.0017	-25.0017	-0.0038	24.9983	-24.9985	24.9985

Stage Unit B

n	intf 0	intf -	intf 0	intf +	enc -	enc +
1	-0.0010	-24.9980	-0.0020	24.9980	-24.9985	24.9985
2	0.0010	-24.9974	-0.0020	24.9980	-24.9985	24.9985
3	0.0010	-24.9980	-0.0020	24.9985	-24.9985	24.9985
4	0.0012	-24.9976	-0.0021	24.9987	-24.9980	24.9990
5	-0.0005	-24.9978	-0.0019	24.9983	-24.9980	24.9990
6	0.0006	-24.9979	-0.0019	24.9984	-24.9985	24.9985
7	0.0005	-24.9980	-0.0021	24.9984	-24.9985	24.9985
8	0.0004	-24.9980	-0.0018	24.9985	-24.9985	24.9995
9	0.0007	-24.9979	-0.0020	24.9985	-24.9985	24.9985
10	0.0013	-24.9973	-0.0014	24.9989	-24.9975	24.9985

Figure 18: Comparison of laser interferometer and linear encoder

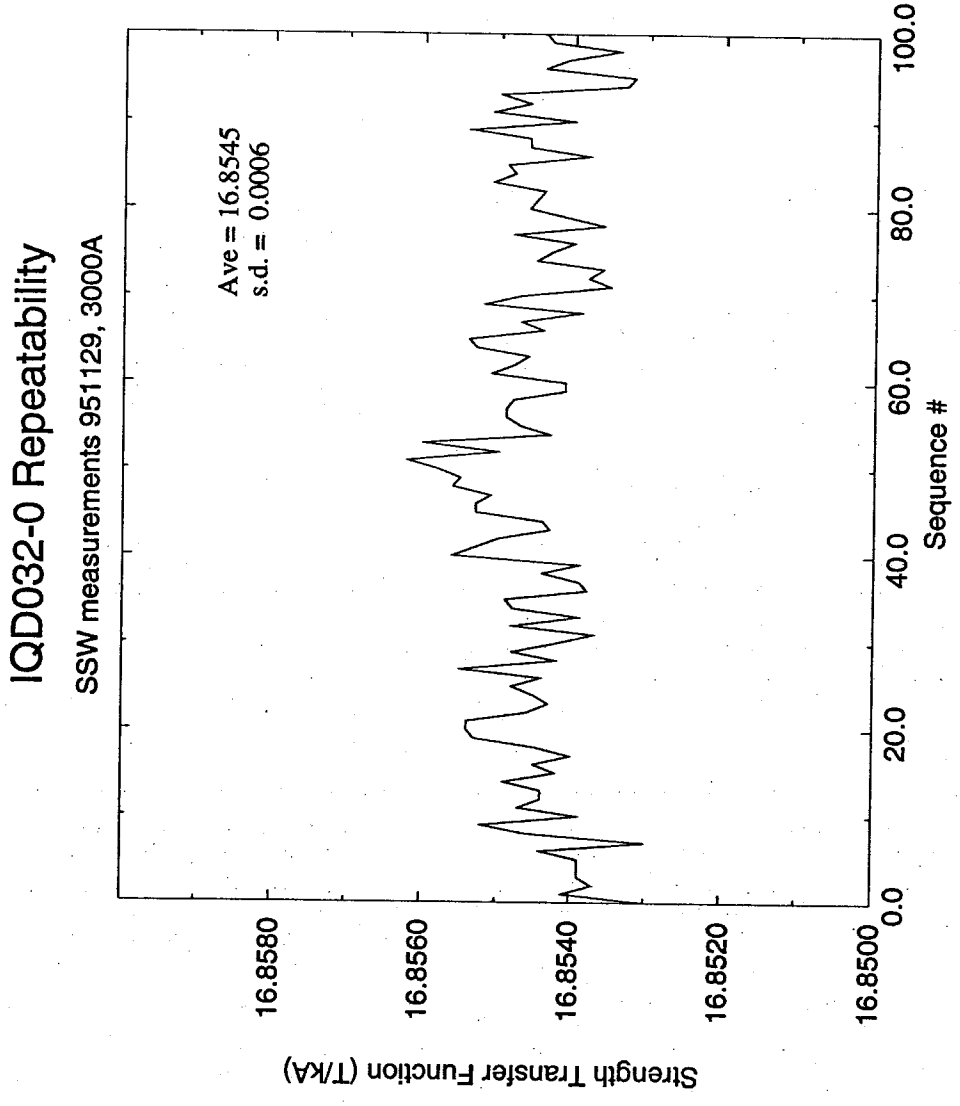

Figure 19: Integral Strength TF repeatability at 3kA

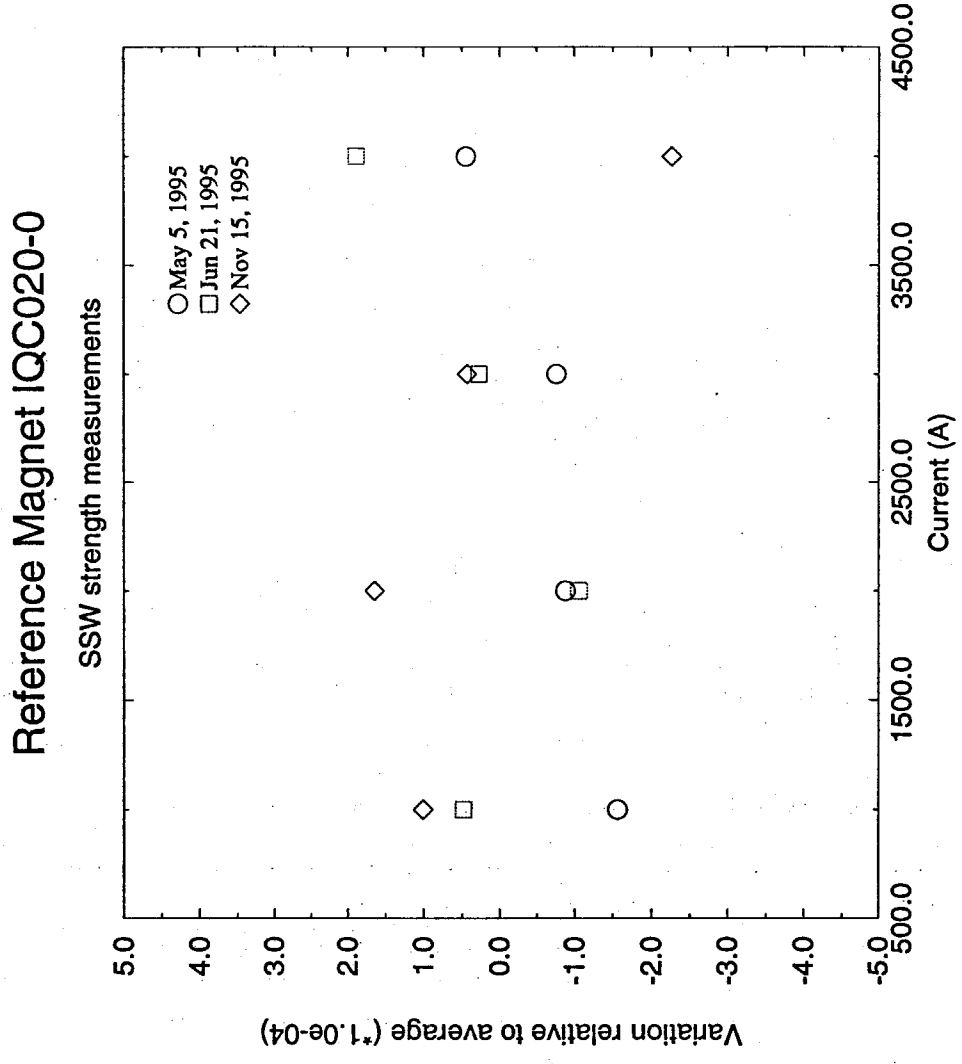

Figure 20: Long term repeatability using reference magnet

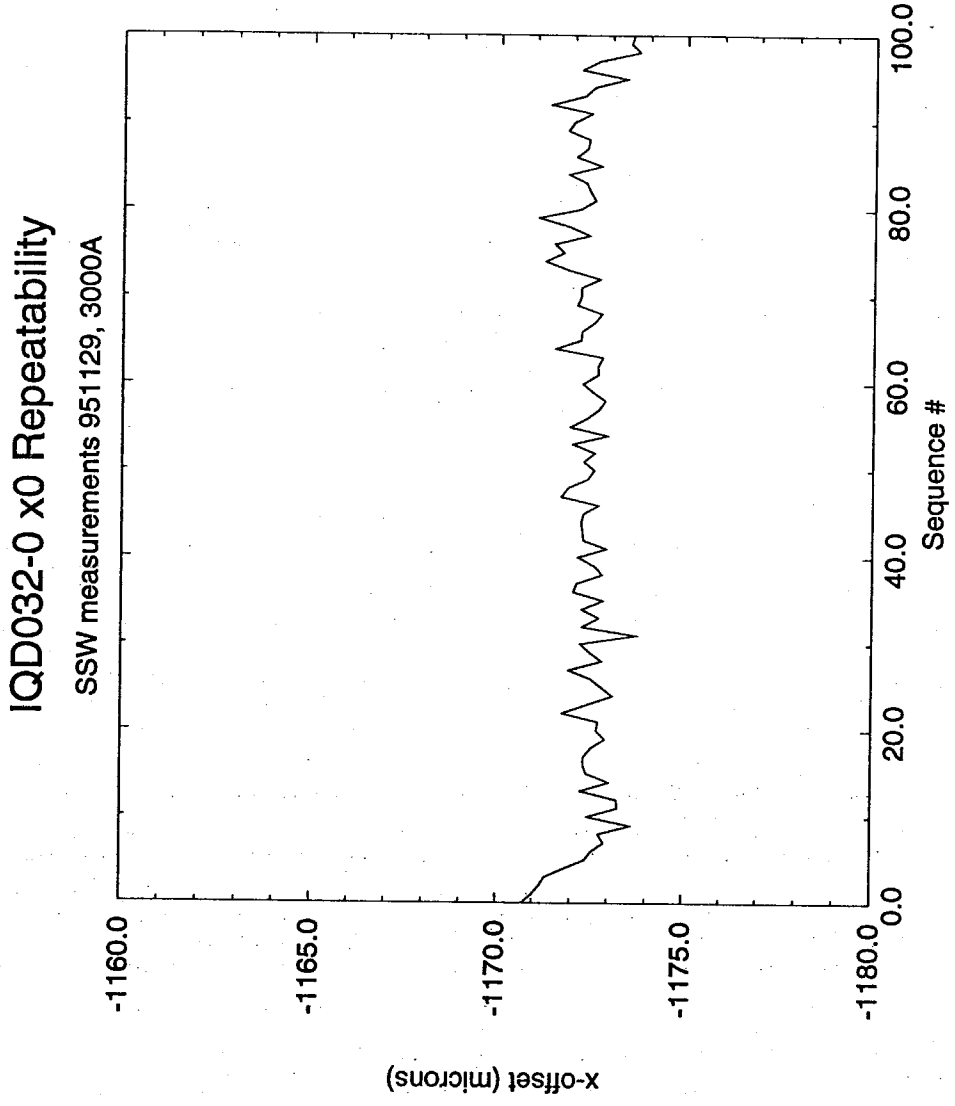

Figure 21: Repeatability of x-center measurements

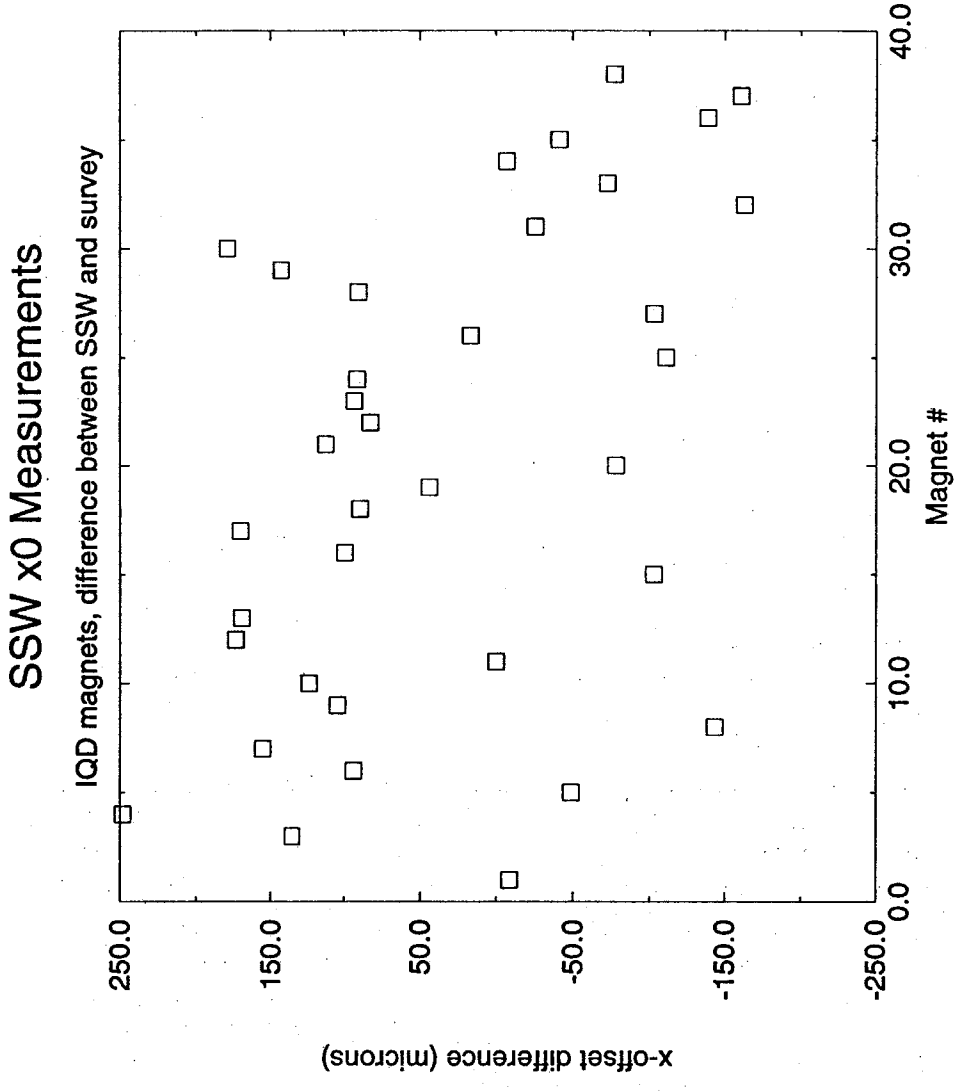

Figure 22: Comparison of survey and SSW x-center measurements

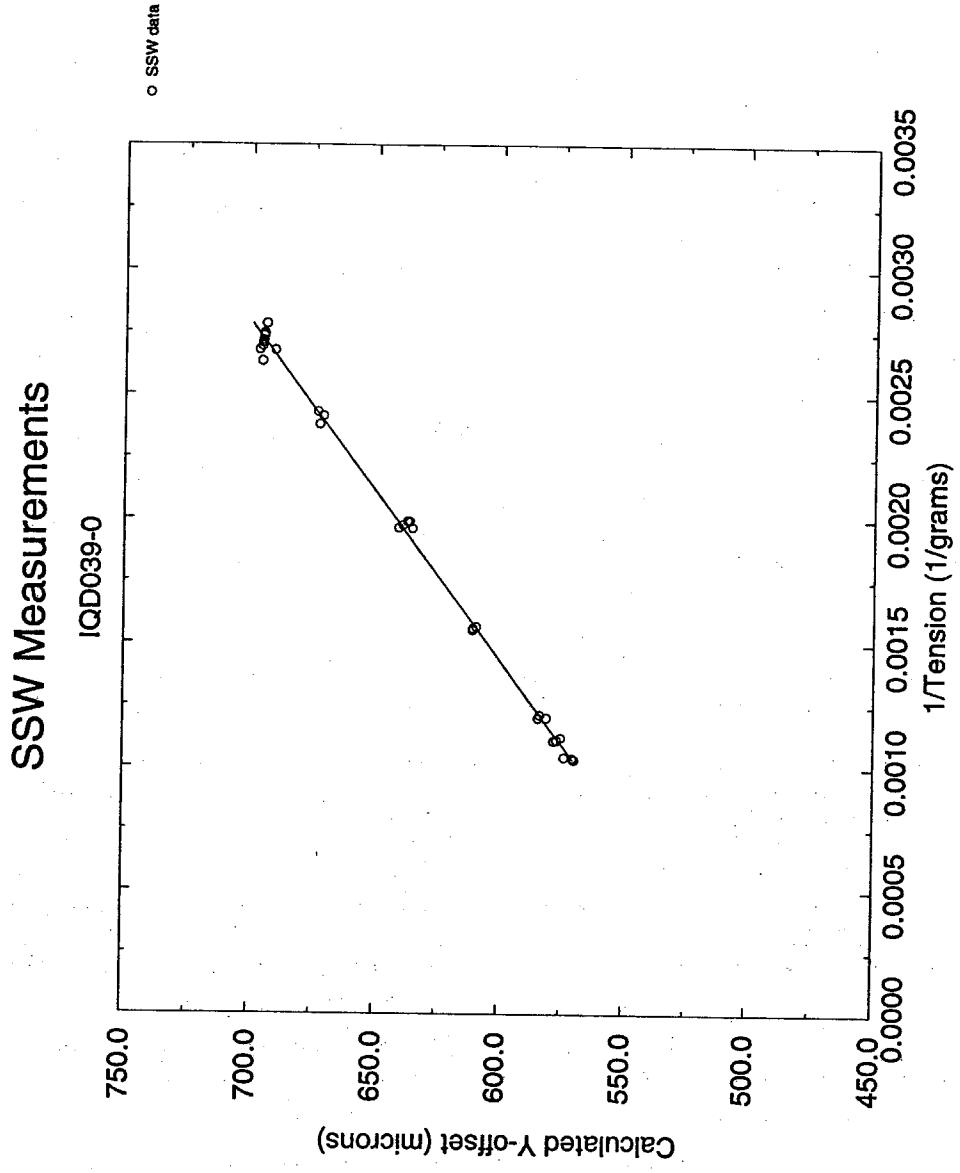

Figure 23: Measurements of y-center as a function of tension

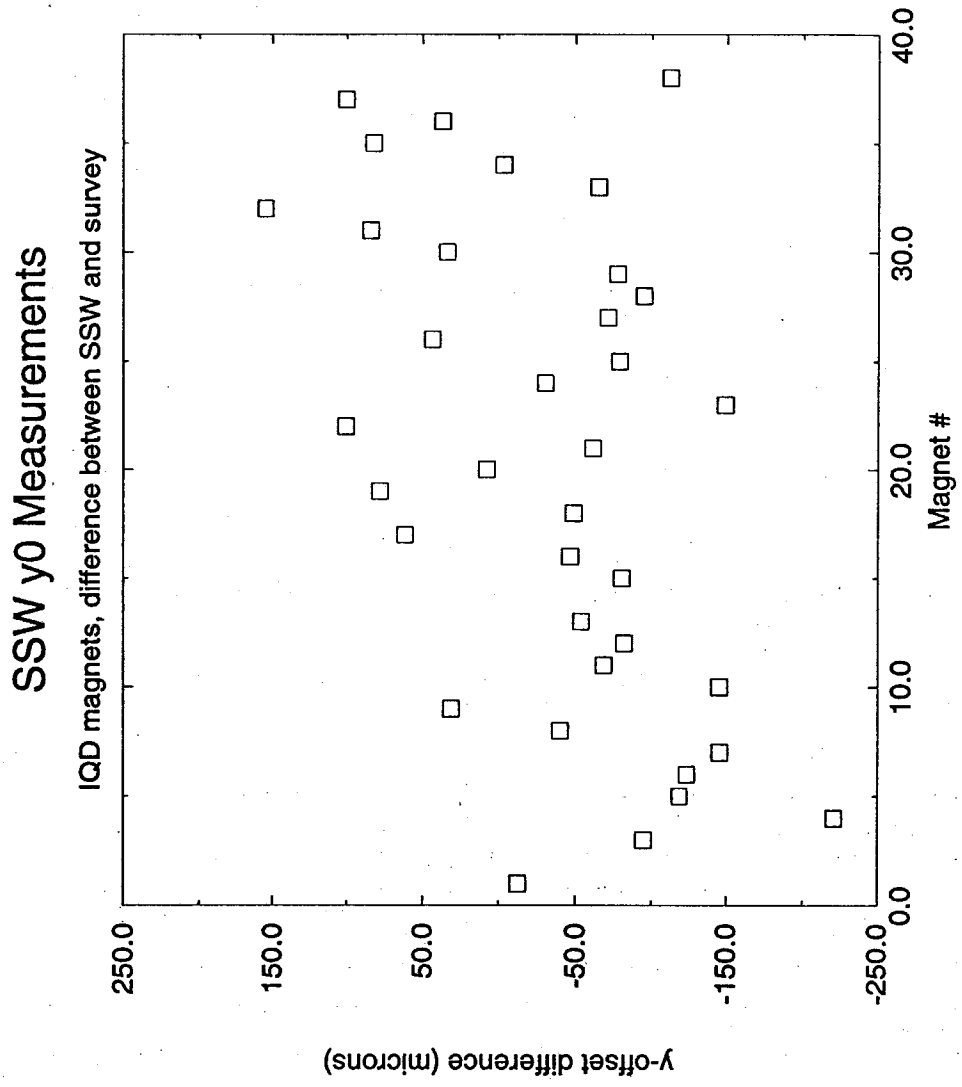

Figure 24: Comparison of survey and SSW y-center measurements

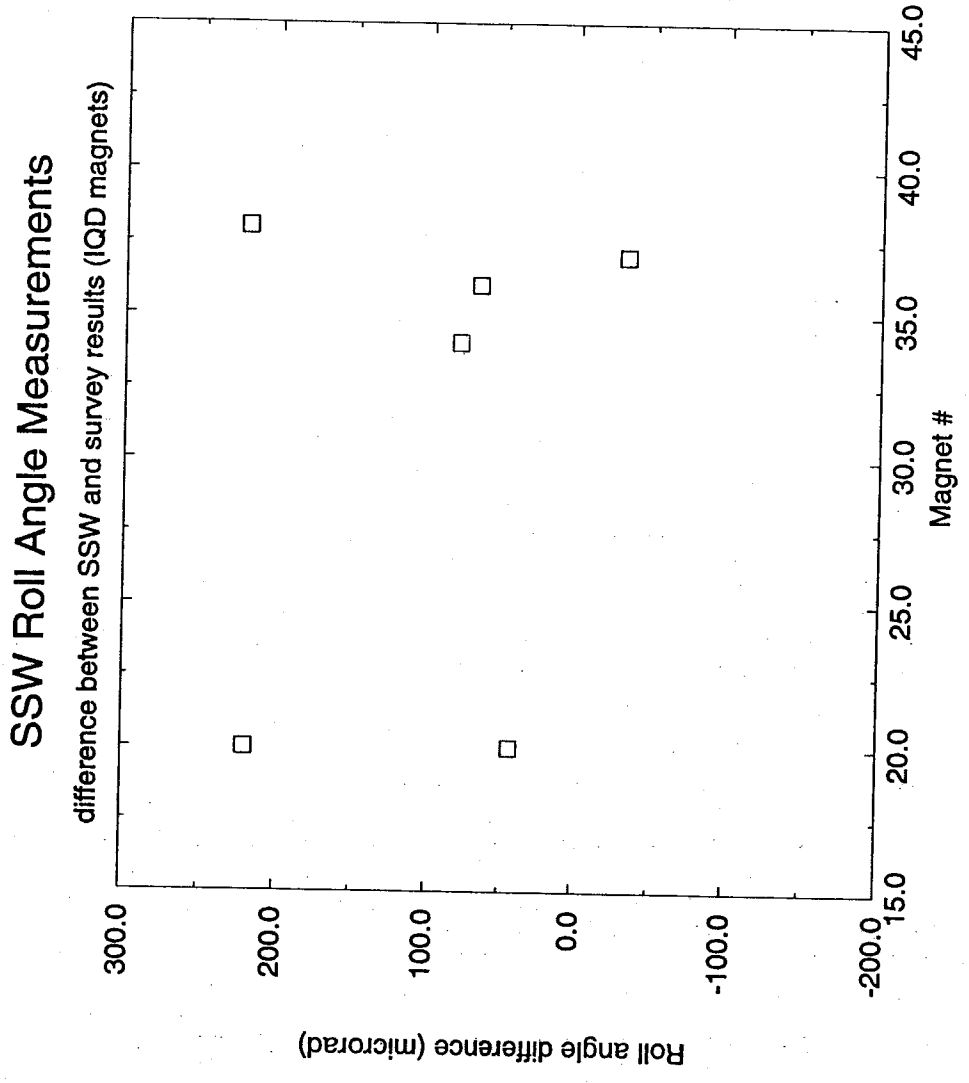

Figure 25: Comparison of survey and SSW roll angle measurements

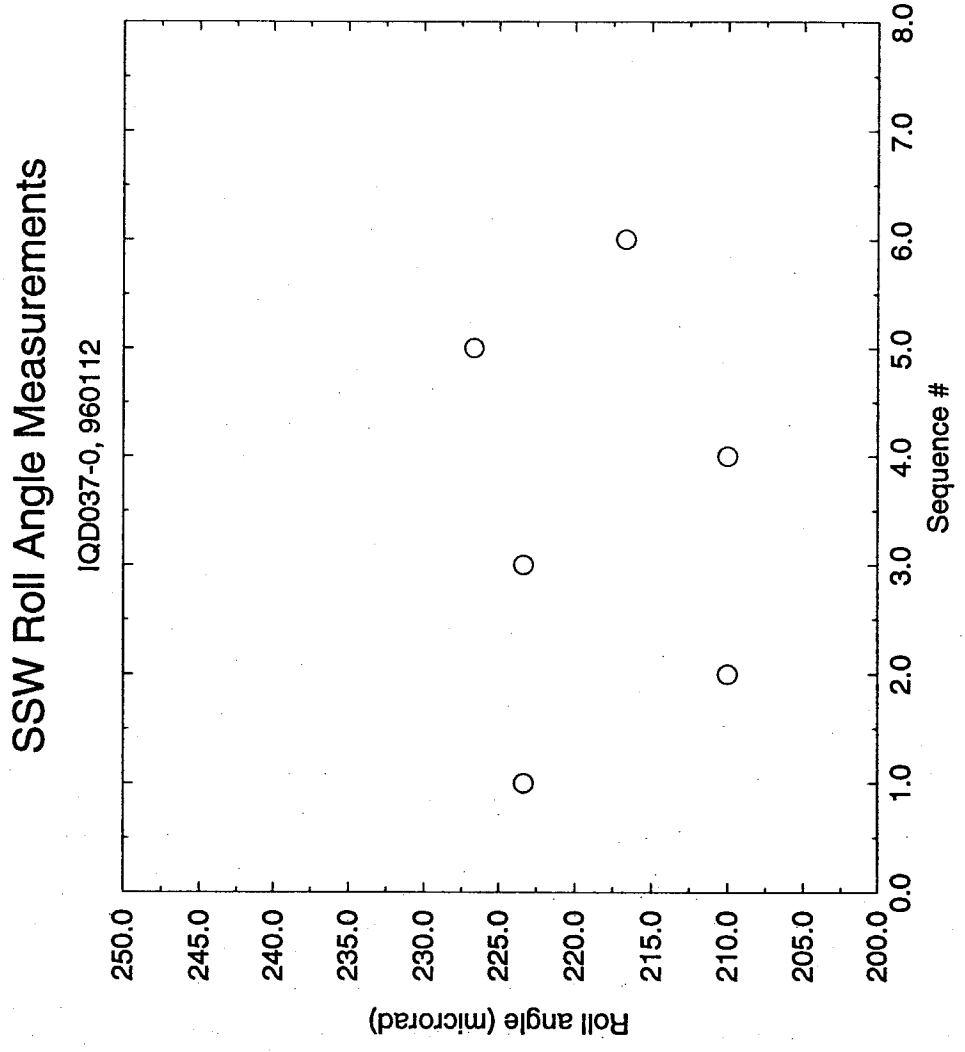

Figure 26: Repeatability of SSW roll angle measurements